

X-692-75-33  
PREPRINT

NASA TM X-70842

# MAGNETIC FIELD OF THE MAGNETOSHEATH

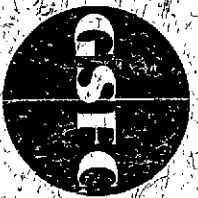
N75-18825

(NASA-TM-X-70842) MAGNETIC FIELD OF THE  
MAGNETOSHEATH (NASA) 70 P HC \$4.25 CSCL 03B

G3/46 Unclas  
13295

D. H. FAIRFIELD

JANUARY 1975



———— GODDARD SPACE FLIGHT CENTER ————  
GREENBELT, MARYLAND

**For information concerning availability  
of this document contact:**

**Technical Information Division, Code 250  
Goddard Space Flight Center  
Greenbelt, Maryland 20771  
(Telephone 301-982-4488)**

**"This paper presents the views of the author(s), and does not necessarily  
reflect the views of the Goddard Space Flight Center, or NASA."**

MAGNETIC FIELDS OF THE MAGNETOSHEATH

by

D. H. Fairfield  
Laboratory for Extraterrestrial Physics  
NASA/Goddard Space Flight Center  
Greenbelt, Maryland

January 1975

Submitted to Reviews of Geophysics and Space Physics

## Abstract

The magnetic field of the magnetosheath is most naturally discussed in terms of its steady state and its fluctuating components. Theory of the steady state field is quite well developed and its essential features have been confirmed by observations. The interplanetary field is convected through the bow shock where its magnitude is increased and its direction changed by the minimal amount necessary to preserve the normal component across the shock. Convection within the magnetosheath usually increases the magnitude still further near the subsolar point and further distorts the direction until the field is aligned approximately tangent to the magnetopause. Fluctuations of the magnetosheath field are very complex, variable and not well understood. Power spectra of the field typically vary as  $1/f$  or  $1/f^2$  below and  $1/f^3$  above the proton gyrofrequency. Spectral peaks are common features which occur at different frequencies at various times. Transverse waves are often dominant at frequencies  $\approx .002$  Hz and compressional waves are often dominant at somewhat higher frequencies. Perturbation vectors of hydromagnetic waves tend to be aligned with the shock and magnetopause surfaces. Magnetosheath waves may be generated upstream, within the magnetosheath, at the bow shock, or at the magnetopause, but the relative importance of these sources is not known.

## TABLE OF CONTENTS

- I. Introduction
- II. Steady State Magnetosheath
  - A. Theory
  - B. Observations
- III. Magnetosheath Time Variations
  - A. General Overview
  - B. Magnetosheath Waves Observations
  - C. Origin of Magnetosheath Fluctuations
    - 1. Upstream Origin
      - a. Wave Transmission
      - b. Discontinuities
    - 2. Shock Generation
    - 3. Magnetopause Origin
    - 4. Magnetosheath Generation
- IV. Summary and Future Work

## MAGNETIC FIELDS IN THE MAGNETOSHEATH

### I. INTRODUCTION

A tenuous totally ionized plasma continually flowing out from the sun is known as the solar wind. Due to its high electrical conductivity, solar magnetic fields are "frozen in" the solar wind and are carried outward to the orbit of earth and beyond. The magnetized solar wind plasma which encounters the earth is diverted by the geomagnetic field, confining the latter to a region known as the magnetosphere. Located upstream from the magnetosphere is a detached bow shock - a thin boundary, upstream of which sound and Alfvén velocities are not large enough to convey information to the incoming plasma about the downstream obstacle. The region bounded by the bow shock on the upstream side and by the outer boundary of the magnetosphere (the magnetopause) on the downstream side is known as the magnetosheath. The steady state and time varying properties of the magnetosheath magnetic field constitute the topic of this review.

Knowledge of the properties of the magnetosheath magnetic field is important in several respects. First, although the mean free path for coulomb collisions is of the order of 1 astronomical unit in the solar wind at the earth's orbit, continuum hydromagnetic theory does a remarkably good job of describing the solar wind - geomagnetic field interaction. Apparently fundamental plasma processes create a scale length very much smaller than the coulomb mean free path causing the plasma to behave like a fluid on a much smaller scale. The magnetic field undoubtedly plays a role in this behavior and its study promises further insight into these basic plasma processes. The magnetosheath appears to be a particularly appropriate region to study such fundamental plasma physics.

Another incentive for studying the magnetosheath magnetic field follows from the many correlation studies which have shown that both the north-south (e.g. Hirshberg and Colburn, 1969), and east-west (e.g. Svalgaard, 1974) components of the interplanetary field are important in regulating the dynamical processes in the earth's magnetosphere. The physical mechanisms producing these correlations are poorly understood and an improved understanding will require a further investigation of how a steady state interplanetary field interacts with the magnetosphere. Convection of the interplanetary field into the magnetosheath is the first stage in this process. The magnetosheath field-magnetosphere field interaction at the magnetopause is the second stage whose detailed understanding is necessary to explain the known correlations. A third reason for studying the magnetosheath field is that some of its fluctuations are generated at the bow shock and the magnetopause. Understanding these waves should yield insight into the physical processes taking place within these boundaries.

Section II of this review discusses the magnetic field of the steady state magnetosphere. The hydromagnetic continuum theory is discussed first, because of its leading role in understanding the steady state magnetosheath. Measurements are then reviewed and found to support the theory.

Section III describes the time varying magnetic fields of the magnetosheath. Emphasis is placed on the measurements which reveal a rich, complex, variety of waves at many different frequencies. To a large extent, wave modes have not been identified and locations where the waves are generated have not been determined. This lack of experimental knowledge has limited the theoretical understanding of the time variations. The possible sources for magnetosheath waves are reviewed.

Section IV summarizes the paper and suggests areas for further investigations.

## II. STEADY STATE MAGNETOSHEATH

### A. Theory

The techniques used for calculating the plasma and field parameters of the steady state magnetosheath are well known and excellent reviews exist (e.g. Spreiter et al., 1968; Spreiter and Alksne, 1969). Such studies investigate the flow past an axi-symmetric body which is usually obtained by rotating the equatorial trace of the magnetosphere boundary. A more realistic shape representing indentations at the "neutral points" in the polar regions might give rise to a second shock wave within the magnetosheath (Walters, 1966), but only one tentative observation of such a shock has been reported (Scarf et al., 1974). In this paper we will briefly review only those aspects of the theory which lead to determinations of the magnetic field of the magnetosheath.

The full set of magnetohydrodynamic equations for the steady flow of a dissipationless perfect gas (e.g. Spreiter et al., 1966a) can only be solved exactly in the case when the interplanetary field is aligned with the solar wind direction. (The earth-sun line is assumed to be the solar wind flow direction in all theoretical work). Results in this special case (Lees, 1964; Dryer and Faye-Petersen, 1966; Spreiter et al., 1966a; Dryer and Heckman, 1967) are illustrated in Figure 1 (Dryer, 1970) which shows the strength of the magnetosheath field (and equivalently the mass flux) relative to the interplanetary value for four different values of the specific heat ratio  $\gamma$ . Results are quite sensitive to  $\gamma$ , a fact which has allowed experimental determinations of  $\gamma$  which favor a value near 5/3 (Auer, 1974, and references therein). The Figure 1 results for this special field aligned case



show that the magnetosheath field is unity at the shock at the subsolar point (a parallel shock) and reaches a maximum at the shock at a location near the dawn-dusk meridian plane. The field goes to zero at the stagnation point (the intersection of the magnetopause and the earth-sun line) where plasma pressure alone must balance the pressure of the geomagnetic field. In this special field aligned case, all quantities exhibit axial symmetry about the flow direction and field lines are identical to stream lines.

The field aligned case may be contrasted with another special case where the field is transverse to the solar wind direction. Lees (1964) has solved this problem in two dimensions where variations are not permitted in the direction perpendicular to the plane of the field and the earth-sun line. He finds that the field magnitude along the earth-sun line increases at the shock and reaches it's maximum value at the stagnation point. The Lorentz force deflects the flow and prevents any plasma from reaching the stagnation point where the density is zero. Magnetosheath magnetic field pressure alone must balance the geomagnetic field at the stagnation point in this case.

To calculate the magnetosheath magnetic field for more arbitrary field orientations, it has generally been necessary to use the fact that the kinetic energy of the solar wind is much greater than its magnetic energy. Under these conditions (equivalently stated as large Alfvén mach number conditions), the equations decouple into a gas dynamic set and an electromagnetic set (Spreiter et al., 1966a). The gas dynamic equations for flow past an axisymmetric blunt body (the magnetosphere) are then solved for the fluid parameters in the magnetosheath. These parameters are illustrated in Figure 2 (Spreiter et al., 1966b) for the case with an upstream gas dynamic mach number ( $M_\infty = \frac{V_\infty}{a_\infty}$  where  $V_\infty$  is the upstream plasma velocity and  $a_\infty$  is the upstream sound velocity) of 8.71 and  $\gamma = 2$ . Shown are magnetosheath contours of the velocity  $V$ , mass flux  $\rho V$ , density  $\rho$  and temperature  $T$ . As

plasma flows into the magnetosheath in the subsolar hemisphere it is compressed ( $\rho/\rho_\infty \simeq 3$ ), the kinetic energy is decreased ( $V/V_\infty \simeq .3$  to  $.7$ ) and converted into random energy ( $T/T_\infty \simeq 15$  to  $30$ ). As the plasma continues its flow past the magnetosphere, the process reverses with temperatures decreasing and velocities increasing as thermal energy is converted back to kinetic-energy. Calculation of the magnetic field is then accomplished by considering the previously neglected electromagnetic equations  $\nabla \times (\vec{B} \times \vec{V}) = 0$  and  $\nabla \cdot \vec{B} = 0$  and  $B_{n1} - B_{n2} = 0$ , where  $B_{n1}$  and  $B_{n2}$  are the field components normal to the bow shock on the upstream and downstream sides respectively. For any given upstream field the latter condition along with the previously calculated plasma quantities determines the field adjacent to the shock on the downstream side. The  $\nabla \times (\vec{B} \times \vec{V}) = 0$  equation is the mathematical expressions for the frozen field condition. Since this frozen field is convected with the plasma it is possible to use the previously calculated magnetosheath velocities and integrate  $\vec{V} dt$  over a fixed time  $\Delta t$  to find the subsequent location of a plasma element with its associated field line. By successively carrying out this procedure for many points, the three dimensional-steady state-vector magnetic field of the magnetosheath can be determined with an accuracy that in principle is limited only by the original high mach number assumption that allowed the decoupling of the equations.

Several investigators have used this technique to calculate field lines in the magnetosheath. Spreiter et al., (1966a) considered those cases when the interplanetary field was oriented at  $45^\circ$  and  $90^\circ$  to the flow direction, but they limited their calculation to the symmetrical case where the field-velocity plane passed through the center of the earth. Their results showed how the field lines tend to become draped over the nose of the magnetosphere and compressed against it. Dryer and Faye-Peterson (1966)

obtained similar results in studying the  $90^\circ$  orientation case, but they investigated the interplanetary field lines which lay in the plane defined by the flow velocity and field vector but which passed through the magnetosphere at a distance offset from the center of the earth by a distance  $D/2$  where  $D$  is the geocentric distance to the stagnation point. These calculations indicated distortion of the field in the third dimension. Alksne (1967) used this technique in a more general manner, by considering several oblique orientations in several offset planes. An example of these results are illustrated in Figure 3 (Spreiter et al., 1968) for the case when the interplanetary field makes an angle of  $45^\circ$  with flow direction but where the plane of the field and the flow is offset from the parallel plane through the earth's center (the XY plane) by a distance  $D/3$ . The left hand portion of the figure shows field lines projected in the XY plane and the right hand portion shows the projection in the YZ plane. The intersection of the field plane with the bow shock is designated by a solid line and the intersection with the magnetopause with a dashed line. The numbered contours indicate the field strengths. The XY projection shows that portions of the field lines near the subsolar point where the velocity is low tend to lag behind the portions of the field lines on the flanks, so that the field appears to become draped across the magnetosphere and aligned tangentially to its surface. Compression is greatest in the subsolar region, but is asymmetric, with fields in the dusk hemisphere having higher magnitudes than those at a symmetrical location in the dawn hemisphere. The YZ projection shows significant distortion of the field in the third dimension. The several specific examples of field distortions calculated by Alksne have been presented in a more general form by Alksne and Webster (1970).

Shen (1972) advanced the fluid theory by solving the magneto-hydrodynamic equations without neglecting the magnetic field terms and decoupling the equations. His analysis is performed for several oblique orientations of the interplanetary field but is again confined to a symmetrical case where the plane of  $B$  and  $V$  includes the earth-sun line. Inclusion of the oblique magnetic field means that Shen's results are the first to give asymmetries in the magnetosheath plasma parameters, although Walters (1964) had proposed such asymmetries after evaluating the conservation relations across the bow shock. Shen evaluates the pressure at the magnetopause in an effort to determine magnetopause asymmetries such as had been proposed by Walters. He confirms the finding of Walters that dawn side plasma pressure exceeds that on the dusk side, but he goes on to point out that the magnetic field asymmetry is in the opposite direction so that the total pressure near dusk is greater than that near dawn. Hirsh and Reshotko (1971) also show that the effect proposed by Walters would be confined largely to the region near the subsolar point, thus making it less effective in creating a magnetospheric asymmetry than was originally thought.

The magnetosheath fields calculated by Shen are not greatly different than those given by Alksne (1967) which is not surprising since Shen's velocity asymmetries are not large, with symmetric locations showing differences of not more than 20%. Alksne's large three dimensional field distortions would seem to be more appropriate for comparison with experiment than Shen's mathematically more exact two dimensional results.

#### B. Observations

The most extensive observations of the steady state fields in the

magnetosheath have been made by the Explorer or IMP class spacecraft. Simultaneous measurements by IMP 1 and IMP 2 (Fairfield, 1967) demonstrated the essential validity of the frozen field approximation. Whenever IMP 1 detected a discontinuity in the interplanetary medium, IMP 2 detected the a similar discontinuity further downstream a few minutes later with a time delay which was consistent with convection from one spacecraft to the other at the plasma flow velocity. This type of data is illustrated in Figure 4 (Behannon and Fairfield, 1969) which displays simultaneous data when Explorer 34 was in the interplanetary medium near the Earth-Sun line  $32R_E$  (earth radii) upstream from the Earth while Explorer 33 was in the dusk magnetosheath  $45 R_E$  downstream from the Earth. In the figure,  $F$  denotes the field magnitude,  $\theta$  the latitude angle of the vector field in solar ecliptic coordinates and  $\phi$  the longitude angle with  $90^\circ$  representing a field directed from dawn to dusk. Angular changes such as those in  $\phi$  near 22:00 and in  $\theta$  at 23:15, 00:50 and 1:40 are seen at Explorer 34 approximately 10 minutes before they are seen at Explorer 33. In principle it is possible to compute a velocity by dividing the spacecraft separation by the observed time delay. Agreement of this velocity with a measured plasma velocity would indicate strict validity of the frozen field approximation, whereas, disagreement would indicate propagation of the discontinuity relative to the streaming plasma. In practice, the two spacecraft usually are not aligned along a radial vector from the sun, so they do not measure the same volume element of plasma. Under these circumstances it is necessary to know the three dimensional shape and orientation of the discontinuity surface to compute the expected arrival time under the frozen field assumption. In practice it is difficult to determine these quantities with enough accuracy to allow determination of any propagation relative to the plasma. (Burlaga and Ness, 1969).

Utilizing one opportunity when Pioneer 7 was  $1000 R_E$  (earth radii) behind the earth, good agreement was found between a velocity calculated from the transit time and the simultaneously measured solar wind velocity (Fairfield, 1968).

While discontinuities are useful for demonstrating that the interplanetary field is the origin of the magnetosheath field, they are of no further use in evaluating steady state theories which assume a uniform interplanetary field. However, these discontinuities usually occur at intervals of the order of one hour (e.g. Burlaga, 1972) which are long compared to the time it takes an element of plasma to pass the magnetosphere. The field between discontinuities can be supposed to approximate the steady conditions

assumed by theory. Furthermore, simultaneous interplanetary observations at spacecraft separations of a few tens of earth radii generally reveal similar vector fields (Fairfield 1967). This observation demonstrates that the spatial scale for appreciable interplanetary changes is usually large compared to magnetosphere dimensions; to a first approximation, a point measurement in the upstream region can be considered representative of a uniform field on the scale of the magnetosphere.

The simultaneous field measurements by IMP 1 and IMP 2 (Fairfield, 1967) were the first to demonstrate the relation between steady state interplanetary and magnetosheath fields. Figure 5 illustrates magnetosheath fields which have been averaged between discontinuities and are projected in the ecliptic plane. Data in the various panels have been separated according to the direction of the simultaneously measured interplanetary

fields. The vectors tend to be aligned among themselves and also aligned with the magnetopause, in spite of the fact that the azimuth angle  $\phi$  of the simultaneous interplanetary data ranges over  $180^\circ$ . In the left hand panels where  $0^\circ < \phi < 180^\circ$ , the magnetosheath field generally is oriented in the dawn to dusk direction; whereas, in the right hand panels with  $180^\circ < \phi < 360^\circ$  the magnetosheath field tends to be oriented in the dusk to dawn direction. In other words, the sign of the Y component of the interplanetary field is what determines whether the magnetosheath field will point in the dawn or dusk direction.

These observations are further supported by a statistical study of over 340 hours of IMP 2 data in the magnetosheath (Fairfield, 1967). Data from the inner magnetosheath (the half of the subsolar magnetosheath closest to the magnetopause) showed a preponderance of orientations in directions tangent to the magnetosphere and no occurrence of orientations in the direction approximately along the magnetopause normal. This alignment of the field with the magnetopause is in general agreement with the theoretical results shown in Figure 3. This approximate alignment of magnetosheath fields with the magnetopause does not, however, preclude the existence of a small field component across the magnetopause and, hence, the results should not be interpreted as demonstrating that the magnetopause is a tangential discontinuity (Fairfield, 1967).

The field magnitude in the magnetosheath can best be studied by considering the measured magnetosheath field as normalized by a simultaneous measurement of the interplanetary field. Behannon and Fairfield (1969) utilized a total of 1661 such hourly average pairs which were measured by four Explorer spacecraft. The magnetosheath

magnitude  $|B|$  normalized by the simultaneously measured interplanetary magnitude  $|B_0|$  are shown at their position of measurement in the magnetosheath in Figure 6. They are compared with the dashed contours of Alksne (1967) which are labeled by the circled numbers. Measurements are restricted to interplanetary orientations which make angles between  $80^\circ$  and  $90^\circ$  with the earth-sun line and to magnetosheath observation points between 4 and  $15 R_E$  from plane defined by the interplanetary field and the earth sun line. The theory is for the case where the field is perpendicular to the earth-sun line and where the XY plane intersects the Z axis at a distance equal to  $2/3$  of the subsolar magnetopause distance. Experimental values as high as 6.0 occur near the subsolar region and decreases to less than unity in the downstream region. The agreement between experiment and theory appears to be satisfactory considering the rather wide range of experimental Z positions.

The upstream to downstream decrease in  $B/B_0$  seen in Figure 6 is further illustrated in Figure 7. Values from all Y and Z positions and all field orientations are included and the data span the entire range of X values. The average values decrease from 4.0 in the upstream region near the subsolar point to less than unity downstream. Variations between the shock and the magnetopause in any given X region are suppressed in this presentation, but it should be noted that values less than unity are not uncommon in the downstream region away from the shock. This observation is predicted by the theory (e.g. Dryer and Heckman, 1967, Alksne, 1967). When the data of Figure 7 are separated according to interplanetary field orientation, the dawn dusk magnitude asymmetry predicted in Figure 3 is also detected (Behannon and Fairfield, 1969).

Information on the orientation of the field is presented in Figure 8.



Magnetosheath vectors are shown for cases when the interplanetary field makes an angle between  $30^{\circ}$  and  $40^{\circ}$  with the earth-sun line. The XY plane is that defined by the upstream field and the X axis. In the "dusk" hemisphere where the interplanetary field is approximately aligned with the shock surface, the field undergoes a minimal angle change at the shock in order to preserve the normal component across the shock. Fields in the dusk hemisphere are very well ordered. In the dawn hemisphere the field is nearly normal to the shock surface and must undergo a much larger angle change in order to conserve its normal component. Also large amplitude fluctuations tend to be present in the upstream field for these approximately parallel field-shock normal orientations (see next section). The vectors in the dawn hemisphere are less well ordered than those on the dusk side. In the dawn hemisphere apparently the field at the shock is sometimes distorted in one direction to preserve its normal component rather than in the opposite direction as it would be if it were draped across the magnetosphere. The effects of the large amplitude fluctuations may dominate at other times and produce odd orientations.

In summary, the measurements of the average fields in the magnetosheath are consistent with the theoretical predictions of magnetohydrodynamic theory in the high mach number approximation. The interplanetary field is convected through the bow shock where its magnitude is increased and its orientation changed by the minimal amount necessary to preserve the field component across the shock. Convection within the magnetosheath further distorts the field so that it acquires an orientation approximately tangent to the magnetopause and in effect appears to be draped across the

magnetosphere. The magnetosheath to interplanetary field ratio can be as high as approximately 6 near the subsolar point but decreases at more downstream locations and is frequently less than unity anti sunward of the dawn dusk meridian plane. It should be realized that the difficulties involved in comparing theory and experiment are such that a high order of agreement cannot be claimed. The field of the magnetosheath has not been investigated under low mach number conditions where an accurate theory requiring inclusion of the magnetic field would produce rather different results.

### III. MAGNETOSHEATH TIME VARIATIONS

#### A General Overview

The earliest magnetic field observations of the magnetosheath by the spacecraft Pioneer 1 (Sonett et al., 1959; Sonett et al., 1960), Pioneer 3 (Sonett and Abrams, 1963; Sonett, 1963) and Pioneer 5 (Coleman, 1964) were all single outboard traverses attempting to explore the gross nature of the solar wind-earth interaction. (See Wolfe and Intriligator, 1970 for a historical review of these early measurements) The two-axis search coil magnetometers on these spacecraft identified the large amplitude field fluctuations as characteristic of the magnetosheath, but the very limited understanding of the interaction process combined with relatively primitive and limited data sets precluded any definite conclusions as to the properties of the waves. The early earth orbiting spacecraft more fully delineated the nature of the interaction by conducting extensive surveys using full vector measurements (Cahill and Amazeen, 1963; Ness et al., 1964), but even these experiments lacked the necessary sensitivity (Explorer XII) and time resolution (IMP 1) to adequately study magnetosheath fluctuations. The single axis search coil experiment on the earth orbiting Vela 3 space-

craft further characterized the sometimes irregular nature of the fluctuations (Greenstadt et al., 1967) but lack of vector data prevented a definitive study. Further progress was made with the full vector measurements such as those made by the single outbound traverses of Mariner 4 (Siscoe et al., 1967a,b) and Pioneer 6 (Ness et al., 1966) and earth orbiting OGO-1 (Heppner et al., 1967) and Explorer (Fairfield and Ness, 1970) spacecraft. Even up to the present time, the complexity of magnetosheath fluctuations has apparently discouraged extensive investigation and definitive studies determining polarizations and distinguishing wave modes are lacking.

The nature of fluctuating magnetic fields is most conveniently discussed in terms of power spectra (Blackman and Tukey, 1958) where estimates of the power in various frequency bands are plotted versus the frequency. An overview of the magnetosheath is attempted in Figure 9 which displays a composite spectra of the total field magnitude covering 11 decades in power and 4 decades in frequency. The data have been drawn from many sources and illustrate the primary features of magnetosheath fluctuations. The usefulness of Figure 9 is limited by the fact that magnetosheath fluctuations may be very different at various times. (e.g., Fairfield and Ness, 1970, Smith and Davis, 1970).

The most representative spectra in Figure 9 are probably those calculated from thirty minute intervals on Sept. 1 and Nov. 1, 1967 (Fairfield and Ness, 1970). These two spectra were selected from a large number of spectra in the subsolar hemisphere to illustrate typical periods of high and low amplitude fluctuations. The spectra peaks near .05 hz on Sept. 1 and .07 hz on Nov. 1 are typical, but the exact frequency

of the peaks and their magnitude are variable. The Explorer 12 spectrum (Kaufmann et al., 1970) was selected on the basis of very large amplitude fluctuations so it is not surprising that its power level is relatively high. The July 31 spectrum illustrates a period when the interplanetary magnetosonic mach number reached a very low value. Formisano et al., (1971) and Fairfield (1971) have shown that under these conditions and stand off distance of the bow shock increases dramatically to a distance as much as 10 or 15  $R_E$  upstream from the magnetosphere. Under these unusual conditions magnetosheath fluctuations achieve the very low values represented in Figure 9. The flattening of the July 31 spectra above .4 hz is due to the experimental noise level. The Mariner 4 spectrum (Siscoe et al., 1967a) was calculated from a 7 hour period as the spacecraft departed from the earth near the 0400 local time meridian. The relatively low power level is probably due to the fact that it is further downstream than the other spectra. Mariani et al. (1970) have shown that spectral power decreases exponentially in the downstream region with a characteristic distance of the order of 40  $R_E$ . Peaks occur in the Mariner 4 data if short time intervals are investigated, but they tend to blend together when the 7 hour interval is used. The ATS 1 data (Cummings and Coleman, 1968) were taken during a rare interval when the magnetopause had moved inside of the 6.6  $R_E$  radial distance of this spacecraft. Since such earthward magnetopause distances can occur only under exceptional solar wind conditions, it is not surprising that this spectrum exhibits an unusually high fluctuation level. The largest amplitude fluctuations in Figure 9 were measured in the high latitude dayside magnetosheath by OGO-5 on November 1, 1968 when interplanetary and geomagnetic conditions were very disturbed (Scarf et al., 1974). Large fluctuations are probably characteristic of this high latitude region even during more normal

conditions (Fairfield and Ness, 1972) and may be associated with a standing shock within the magnetosheath (Walters, 1966; Scarf et al., 1974). It is interesting to note that the OGO-5 data in Figure 9 were taken upstream of the point tentatively identified as the second shock.

The highest frequency data in Figure 9 come from the search coil experiments on OGO spacecraft and represent fluctuations in components rather than field magnitude. The solid line spectrum at the highest frequencies is an average spectrum calculated from OGO 3 waveform data obtained several minutes downstream from 11 shock crossings (Olson et al., 1969). Superposed on this data are bars which span the range of values for three sample magnetosheath spectra presented by Smith et al., (1967). A pair of lines representing spectra from OGO 1 correspond to highly disturbed and moderately disturbed intervals within the magnetosheath (Holzer et al., 1966). Dashed lines with slopes of  $1/f$  and  $1/f^3$  are included in Figure 9 for reference. The  $f^{-3}$  variation of spectra in the high frequency region is common but variations in shape and magnitude often occur (Smith et al., 1967). A prominent feature of Figure 9 is the steepening of the spectra in the frequency range above the proton gyrofrequency. This feature was pointed out by Siscoe et al. (1967a) and Smith et al. (1967) and is probably due to the cutoff of slow magnetoacoustic wave modes at the proton gyrofrequency (see below).

#### B. Magnetosheath Wave Observations

In any investigation attempting to determine the mode of the propagating waves it is useful to know the propagation direction of the waves. A technique for determining this direction (except for an ambiguity in sign) was first used by Siscoe et al. (1967b) who adapted an approach previously used to study discontinuities at the magnetopause (Sonnerup and Cahill, 1967) and in interplanetary space (Siscoe et al., 1968). The technique involves a minimization of the quantity  $\sum_{n=1}^N (\vec{B}^i \cdot \vec{n})^2 = s^2$

where the  $\vec{B}^i$  are N vector field measurements. This problem is equivalent to determining the three eigenvalues of the real symmetric matrix

$$T_{\mu\nu} = \sum_{i=1}^N B_{\mu}^i B_{\nu}^i \quad \mu, \nu = X, Y, Z$$

The eigenvectors associated with the eigenvalues, denoted  $s_k^2 \leq s_{\ell}^2 \leq s_m^2$ , define a coordinate system where  $\hat{k}$  is the direction of minimum variance,  $\hat{m}$  is the direction of maximum variance and  $\hat{\ell}$  completes the orthogonal system. If plane waves are present,  $\hat{k}$  may be associated with the wave propagation vector, with the perturbation vector lying in the  $\ell m$  plane.

The first use of this technique established the presence of shock-aligned oscillations in the outer portion of the magnetosheath during the single outbound pass of the Mariner 4 spacecraft (Siscoe et al., 1967b).

Siscoe et al. considered 4.8 second intervals of data which occurred every 12.8 seconds and contained four vector measurements. They found that when the spacecraft was downstream and within 15 minutes of the bow shock during several multiple crossings, the fluctuations were often planar in the sense that  $S_k/S_{\ell} < 1/4$ . Since power in the field components was greater than that in the field magnitude by approximately a factor of 3, the perturbation vectors also tended to be approximately transverse to the average field. Furthermore, the associated  $\hat{k}$  directions for the different intervals were distributed in the general direction of the shock normal expected on the basis of gas dynamic theory. This fact implies that the fluctuations were primarily in the plane of the shock surface. In the adjacent low field regions upstream of the shock, planar fluctuations were not so evident.

This tendency for the perturbation vector to align itself with the shock surface was subsequently shown to be a general characteristic of the subsolar magnetosheath and also true at lower frequencies (Fairfield and Ness, 1970). Fairfield and Ness computed power spectra for the field

components perpendicular to the average field for half hour intervals on many passes of IMP 4 through the subsolar magnetosheath. Since the average magnetosheath magnetic field tends to align itself along the shock or magnetopause surface, when one of the directions perpendicular to the average field is oriented near the shock normal the other tends to align itself with the shock surface. In Figure 10, the ratio of the integral powers in the frequency range .01-.2 hz for the components X and Y perpendicular to the average field are plotted versus the angle between the X axis and a model shock normal. When this angle is small (i.e. X is aligned along the shock normal), the power tends to be in the Y component which is aligned with the shock plane. When the angle is large and X is aligned within the shock plane, X contains more of the power. Frequently these fluctuations were linearly polarized but occasionally they were found to be circularly polarized. The alignment of the fluctuation vector with the shock surface is also consistent with a study of the downstream magnetosheath (Mariani et al., 1970) which demonstrated that not only did power transverse to the field vector dominate the power in the field magnitude, but that the greatest power was in the  $Z_{SE}$  component which was approximately parallel to the bow shock and magnetotail boundary at the spacecraft location.

Siscoe et al. (1967a) also noted the presence of large amplitude waves which occurred primarily in the field magnitude in the inner portion of the magnetosheath during the Mariner 4 traversal. Kaufmann et al. (1970) later studied large amplitude waves in this region using data from the Explorer XII spacecraft. The  $12.1 R_E$  apogee of Explorer XII limited the study to the inner magnetosheath and the large digitization error of the experiment ( $\pm 12\%$ ) confined the study to large amplitude events. Kaufmann

et al. considered 12 intervals of the order one hour in length and were able to determine a representative minimum variance direction for eight events. They concluded that the fluctuations in the frequency range .01 to .1 hz tended to be confined to a plane and primarily to a given direction within the plane. They then computed power spectra of two quantities. The first quantity was the field magnitude in the plane perpendicular to the minimum variance direction which they found to be nearly the same as the spectrum computed from the total field magnitude. Their second quantity was the angle  $\xi \equiv \tan^{-1}(B_m/B_\perp)$  where  $B_m$  and  $B_\perp$  are the instantaneous measurements of the components perpendicular to the minimum variance direction.  $\xi$  has the advantage of being affected by rotational waves but not magnetoacoustic waves; however, it has the disadvantage of not having the units of  $\gamma^2/\text{hz}$ . Kaufmann et al. felt the advantage outweighed this disadvantage which they overcame by a conversion of  $\gamma^2/\text{hz}$  units which made the instrumental noise levels of the field magnitude and angular spectra agree.

At the lowest frequencies Kaufmann et al. found that the  $\xi$  spectra rose rapidly with decreasing frequency, indicating the predominance of rotational Alfvén waves with periods longer than about 10 minutes. On the outbound pass of Mariner 5 Smith and Davis (1970) noted the presence of similar linearly polarized waves oscillating parallel to the magnetopause with periods of approximately 2 minutes.

In the higher frequency range of .01 - .1 hz, Kaufmann et al. found greater power in spectra of the magnitude component in the  $\perp m$  plane, thus identifying the waves as magnetoacoustic. Furthermore, the fluctuations seemed to anticorrelate with plasma flux, thus identifying the mode as slow magnetocoustic rather than fast magnetocoustic.

In the later paper, Kaufmann and Horng (1971) considered the waves



in terms of the deviations of the field direction from tangency to the magnetopause. They concluded that plasma clouds or condensations with scales of several hundred to several thousand km are associated with the weak field regions where deviations from tangency are greatest. Cloud dimensions were thought to be extended along the average field direction. These clouds and the distorted field convecting past the spacecraft then produced the waves seen by the spacecraft. Large amplitude waves were found to be particularly prevalent near the earth-sun line.

An example of these waves is given in Figure 11 which displays one minute of data from the IMP 6 spacecraft in an orthogonal coordinate system where the Z axis is aligned along the model magnetopause normal and the Y axis is the average field direction in the XY plane calculated over a fifteen minute interval. The data, taken on an inbound pass through the magnetosheath which closely paralleled the earth-sun line, clearly showed large amplitude waves with a frequency of approximately .05 hz which appear primarily in the field magnitude. Similar waves persist for the entire pass although there appears to be a tendency for their amplitude and period to increase nearer the magnetopause. The average direction of the interplanetary field measured simultaneously by the IMP 5 spacecraft was unusually steady during the 2-hour interval of the IMP 6 magnetopause traversal, oriented approximately transverse to the earth-sun line ( $\phi=100^\circ$ ) and pointing in a slightly southward direction ( $\theta = -23^\circ$ ). The minimum variance direction throughout the magnetosheath is approximately along the earth-sun line (or equivalently the magnetopause normal) and hence is approximately perpendicular to the

average field in the magnetosheath ( $\phi=90^{\circ}$ ). The maximum eigenvector direction is not greatly different from the average field direction.

Composite spectra for both the magnetosheath and the simultaneously measured interplanetary field are shown in Figure 12 along with a sketch of the spacecraft locations. On the left are the X and Y spectra for components perpendicular to the average field direction and on the right are the spectra of the field magnitude. The Y spectra are given by solid lines and the X spectra by dashed lines with the higher power levels corresponding to the magnetosheath. The time interval refers to that of the lowest frequency spectra while the higher frequency spectra were computed from representative shorter intervals. The predominant feature of the spectra is the peak at .06 hz corresponding to the waves in Figure 11. This peak is larger in F than X or Y as it would be for the waves studied by Kaufmann et al. Another striking feature of Figure 12 is the relative power levels of X and Y components at lower frequencies. Not only are the interplanetary X and Y components comparable at low frequencies but the X component in the magnetosheath is not enhanced relative to this level. The Y component, which is in the plane of the shock surface, is enhanced by more than an order of magnitude and is thus in agreement with the results of Figure 10. There is no suggestion of .06 hz interplanetary waves related to the magnetosheath peak, although a small gap at the IMP 5 spin frequency makes this conclusion somewhat tentative.

In the frequency range above 1 hz the information on the magnetosheath field fluctuations comes almost exclusively from the search coil experiments on the OGO 1, 3, and 5 spacecraft. These experiments (Holzer et al., 1966; Smith et al., 1967; Olson et al., 1969; Smith et al., 1969) produced data

on the intensity of fluctuations in broad band channels centered on 5 frequencies between 10 and 1000 hz. Additional waveform data contained information up to a cutoff frequency which was as high as 139 hz on rare occasions when the OGO 5 spacecraft was in a high bit rate telemetry mode.

Data from the 5 spectrum analyzer channels on OGO-3 are presented in Figure 13 for a representative inbound pass on Nov. 21, 1966 (Smith et al., 1969). The magnetosheath is evident as a region of enhanced noise bounded by the much quieter interplanetary and magnetosphere regions. The noise is seen to be broadband in nature since four and sometimes five frequency channels vary in the same manner. The intensity varies considerably with time and order of magnitude changes lasting a few minutes to tens of minutes are common (Smith et al., 1967). The noise is usually higher nearer the boundaries, particularly the bow shock (Holzer et al., 1966). The data of Figure 13 were taken when the instrument was in a high gain mode which caused large fluctuations to saturate the analyzer. For this reason the largest values, particularly in the V(100) channel, are truncated at 5 volts which is below their true value. The 800 hz channel is typically somewhat lower than the other channels, probably due to the fact that 800 hz is generally above the electron gyrofrequency which is a cutoff frequency for wave propagation.

In addition to the broadband noise with a  $1/f^3$  spectral shape discussed above and shown in Figure 9, Olson et al., (1969) report the sporadic occurrence of quasi-monochromatic bursts throughout the magnetosheath on most orbits. The bursts typically occur in the frequency range 50-200 hz and have durations from less than one second to tens of seconds. The

amplitudes are typically tenths of gammas and they are elliptically polarized. The authors tentatively suggest a cyclotron instability involving electrons and whistler mode waves as the most likely explanation of these bursts. Further resolution of this question must await answers to such questions as the left or right hand sense of the polarization, the direction of propagation, and information on the particle anisotropies which are required to feed energy from particles to waves.

As yet no information is available on the relation between  $>1$  hz waves in the magnetosheath and the simultaneous presence and variations of lower frequency waves, plasma and energetic particles. The study of such questions could undoubtedly go a long way towards understanding the nature of the fluctuations.

### C. Origin of Magnetosheath Fluctuations

Before considering the origin of magnetosheath waves it is important to appreciate the relation between the frequency of a wave in the plasma frame of reference and the doppler shifted frequency observed by the spacecraft. To investigate the relative velocities of propagation and plasma flow, we follow the discussion of Smith et al., (1967) and in Figure 14 plot phase velocity as a function of frequency for the two simple modes that can propagate along a magnetic field ( $\theta_k = 0$ ) and the one mode that can propagate across the field ( $\theta_k = 90^\circ$ ). At low frequencies, all three phase velocities are asymptotic to the Alfvén velocity which is 157 km/sec for the typical magnetosheath parameters used. The fast mode waves propagating along the field can exist at any frequency below the electron cyclotron frequency and their phase velocity is an increasing function of

frequency up to a maximum of 3370 km/sec which occurs somewhat below the electron cyclotron frequency. The slow mode propagating along the field exists only below the ion cyclotron frequency and its phase velocity decreases with increasing frequency. The fast mode propagating across the field exists only below the lower hybrid frequency and its phase velocity decreases on approaching this frequency. Also indicated in Figure 14 are typical magnetosheath flow velocities of 100 to 300 km/sec which will be different at different times and at different locations in the magnetosheath.

The doppler shifted frequency observed by the spacecraft,  $\omega_D$  can be written as

$$\omega_D = \omega + \vec{k} \cdot \vec{V}$$

where  $\omega$  is the frequency in the plasma frame,  $k$  is the propagation vector of the wave, and  $V$  is the shocked solar wind plasma velocity relative to the spacecraft whose velocity ( $\sim 1$  km/sec) is neglected. The last term in this equation is the contribution due to motion of the plasma relative to the spacecraft. Defining  $\alpha$  as the angle between  $K$  and  $V$  and using the definition of phase velocity

$V_{ph} = \frac{\omega}{k}$  we may write the above equation as

$$\omega_D = \omega \left( 1 + \frac{V}{V_{ph}} \cos \alpha \right)$$

In the high-power hydromagnetic region below the ion gyrofrequency, we can see from Figure 14 that ( $V_{ph} \simeq V_A$ ). Furthermore, we note in Figure 14 that  $V_A \simeq V$  which indicates that the contribution to the observed frequency due to plasma motion is often comparable to the plasma frame frequency as long as the propagation is not approximately transverse to the flow direction. On the other hand, it appears that the flow velocity

will seldom be more than a factor of 2 or 3 greater than the phase velocity so the observed frequency will seldom be different from the plasma frame frequency or more than a factor of 3 or 4. Above the lower hybrid frequency the phase velocity will be considerably greater than the flow velocity and the observed frequency will be nearly equal to the plasma frame frequency.

In many investigations a power spectrum of many waves is often considered rather than an isolated wave, and hence it is of interest to know the effects of doppler shifting on the power spectrum. Siscoe et al., (1967a) has considered this question under the somewhat restrictive conditions of a non dispersive plasma and power which is not a function of propagation direction. They conclude that the slope of the spectrum is unchanged by the doppler shifting, but the absolute power level is changed by a parameter which depends on the slope of the spectra and the ratio of the plasma velocity to phase velocity.

Upstream Origin - One source for at least some magnetosheath time variations are the waves and discontinuities present in the interplanetary magnetic field. When such variations are convected through the bow shock they will be seen in the magnetosheath and contribute to the power in the magnetic field spectrum (Michel, 1967). The nearly simultaneous detection of such field changes by an upstream and downstream spacecraft has been discussed above and illustrated with Figure 4.

In addition to normal ambient interplanetary field variations, low frequency (.01 - .05 hz) quasi-periodic waves are known to exist upstream from the bow shock on field lines that intersect the shock (Fairfield, 1969). It has been suggested (Fairfield 1969; Barnes 1970) that these waves are

generated in the upstream region by protons emanating from the bow shock. Such waves have small velocities compared to the solar wind velocity and hence they are convected back downstream to the shock, passing through it and contributing to the magnetosheath fluctuations.

Examples of these waves can be seen in Figure 15 which illustrates simultaneous data taken by two spacecraft in the vicinity of the bow shock. IMP 5 is inbound in the dusk quadrant while IMP 6 is outbound in the dawn quadrant as shown in the figure insert. The heavy trace illustrates the field magnitude,  $B$ , solar magnetospheric latitude  $\theta$ , longitude  $\phi$ , and 15 sec standard deviation from IMP 6, while the lighter lines illustrate the similar quantities from IMP 5. At the beginning of the interval shown, both spacecraft are upstream of the shock except for brief IMP 5 encounters with the shock at 18:02 and 18:08. At 18:16 the shock moves out past IMP 6 and at 18:38 it reaches IMP 5. The field ( $\phi \simeq 90^\circ$ ) makes a large angle with the shock at each crossing. In each case the magnitude and the standard deviation increases abruptly at the shock and there is a lack of upstream fluctuations. At 20:34, when both spacecraft are near the average shock position, the shock moves earthward and crosses both spacecraft almost simultaneously. From 20:34 to 21:07 while both spacecraft are upstream, the field ( $\phi \simeq 35^\circ$ ) is approximately parallel to the shock normal at IMP 5 but forms a much greater angle with the shock normal at IMP 6. During this interval, large amplitude fluctuations are apparent at IMP 5 but not at IMP 6. After the shock moves out past IMP 5 at 21:07 large amplitude fluctuations persist in the magnetosheath, thus suggesting the possibility that they may be the upstream waves convecting through the bow shock. The disturbed magnetosheath persists until 21:30 when the field suddenly becomes approximately transverse to the earth-sun line. The greatly enhanced standard deviation from 18:24 to 18:36 at IMP 6 in the magnetosheath

is also probably caused by the interplanetary  $\theta$  angle increasing to a value above  $90^\circ$  which undoubtedly causes waves to be present upstream of IMP 6. Upstream fluctuations are not seen at IMP 6 until 23:30 when the field suddenly becomes approximately parallel to the shock normal ( $\theta=130^\circ$ ). This example supports the concept (Greenstadt et al., 1972, and references therein) that there is a critical angle between the field and the bow shock normal such that for angles less than the critical value upstream waves appear and the downstream magnetosheath is disturbed.

A. Wave Transmission - The theory of wave transmission through the bow shock has been investigated by McKenzie and Westphal (1969), Westphal and McKenzie (1969), McKenzie (1970) and Asséo and Berthomieu (1970). These authors assume wavelengths that are large compared to the shock thickness allowing them to proceed with a hydromagnetic fluid theory which does not require knowledge of the shock structure.

McKenzie and Westphal (1969) investigate an Alfvén wave, with propagation vector in the plane of B and the flow velocity, incident on a fast hydromagnetic shock. In this case Alfvén and magnetoacoustic waves are not coupled. They find that two Alfvén waves appear in the downstream region. Under typical solar wind conditions, the transmitted wave has an amplitude approximately three times that of the incident wave and the generated wave has an amplitude roughly equal to the incident wave. Since the wave energy is proportional to the square of the field amplitude, the wave power for Alfvén waves is increased by approximately an order of magnitude. This increase is in general agreement with the increase in the spectral power in the Y component as seen in the simultaneous spectra presented in Figure 12.

McKenzie and Westphal also find that greater amplification factors should be expected under low Alfvén mach number conditions. This fact



appears to be at variance with the unusually quiet magnetosheath conditions observed at the times of low mach numbers. Resolution of this apparent conflict may lie in the fact that the interplanetary field appears to be unusually quiet under low mach number conditions and hence there may be a considerably lower fluctuation level to amplify.

Westphal and McKenzie (1969) investigate the more complicated case of a magnetoacoustic wave incident on the bow shock. Their primary result is that the incident wave is amplified by a factor of 4. This amplification

leads to an increase in the power by a factor of 16 which is greater than that for Alfvén waves and might suggest that magnetoacoustic waves should predominate in the magnetosheath. This supposition is based on the assumption that Alfvén and magnetoacoustic waves are equally prevalent in the interplanetary medium; whereas, in fact in the case of both ambient interplanetary fluctuations (Coleman, 1966) and bow shock associated waves, (Fairfield, 1969) transverse waves are prevalent. In the interplanetary medium this imbalance may be due to more efficient damping of magnetoacoustic waves (Barnes 1966). This damping might also reduce the magnetoacoustic wave level in the magnetosheath.

Asséo and Berthomieu (1970) consider waves incident on a fast shock at an arbitrary angle. In this more general case the modes do not decouple and Alfvén waves can produce magnetosonic waves and entropy waves; magnetosonic waves produce Alfvén and entropy waves, etc. Furthermore, the amplification factors are found to be so strongly dependent on the angle of incidence that the authors suggest that it will be impossible to evaluate the importance of wave transmission without knowing more about  $\vec{k}$  of the incident waves.

Evidence suggesting that bow shock associated waves contribute to magnetosheath fluctuations is presented in Figure 16 (Fairfield and Ness, 1970). The quantity  $\delta$  is an average of standard deviations computed from 8 points taken within 20 seconds; the average being taken over an entire magnetosheath traversal of several hours duration. The abscissa is effectively the longitude of the spacecraft pass through the magnetosheath. Due to the statistical tendency for the interplanetary field to lie along the spiral angle (e.g. Schatten, 1972), interplanetary fields in the dawn to noon region will more frequently make large angles with the shock surface than those in the noon to dusk region and upstream waves will occur more frequently near dawn. The standard deviation in Figure 16 is indeed enhanced near dawn relative to dusk as it would be if upstream waves were transmitted to the magnetosheath. Additional evidence supporting this viewpoint is supplied by Formisano et al., (1973) who found that the maximum amplitude of magnetosheath field fluctuations observed within 1 hour of the bow shock was almost twice as great (7.7 to 3.9) when upstream waves are present as when they were absent.

B. Discontinuities - Interplanetary tangential discontinuities incident on the bow shock are transmitted through the shock but may be modified by the interaction process. In addition, secondary discontinuities may be generated by this interaction along with various waves; all of which contribute to magnetosheath fluctuations. This theoretical problem has been investigated by several workers.

Jaggi and Wolf (1971) have studied the generation of magnetosonic waves in the magnetosheath by weak tangential discontinuities incident on the bow shock. Results of their linear perturbation analysis show that density and velocity perturbations are most effective in producing waves. A 10% density inhomogeneity typically produces a wave in the magnetic field with an amplitude 3% of the total magnetosheath field.

Neubauer (1973) considers the tangential discontinuity-fast shock interaction problem in greater generality by allowing arbitrary orientation of the discontinuity and shock planes and investigating the non-linear theory. Neubauer's results include both the magnetosonic waves of Jaggi and Wolf (discussed in terms of fast reflected shocks or rarefaction waves by Neubauer) and the parallel alignment case studied by Volk and Auer (1974). The theory predicts the orientation of the modified tangential discontinuity and shock, along with the magnitudes of the various field and plasma parameters on either side of these discontinuities. Numerical results for typical parameters show that when the field direction, but not the field magnitude and plasma parameters, vary across the initial discontinuity, the field angle change across the modified discontinuity can be several degrees different from that across the initial discontinuity. As the same time, the field magnitude ratio across the modified discontinuity can be as much as 20% different from its initial value of unity. Cases when the density increases across the incident discontinuity are even more effective in producing propagating disturbances in the magnetosheath (Neubauer, 1974). A shock generated by the interaction would typically have a field increase of the order of 10% when the density changes by a factor of 2 across the original discontinuity. For certain discontinuity orientations which are particularly common in the dawn hemisphere, a generated fast wave in the magnetosheath can propagate ahead of the point where the discontinuity intersects the shock. This generated fast wave can then interact with the bow shock before the interplanetary discontinuity arrives and this situation leads to a breakup of the initial bow shock with a more complicated set of disturbances.

Additional changes in the orientation of a discontinuity during transit through the magnetosheath have been considered by Rigby and Mainstone (1973).

Experimental work on discontinuities in the magnetosheath has not proceeded beyond the type of observations illustrated in Figures 4 and 15 where simultaneous spacecraft observations reveal qualitatively similar discontinuities before and after encountering the bow shock. Recent high quality measurements could probably be used to search for the relatively small additional effects predicted by theory, but such work has not been reported. Although interplanetary discontinuities undoubtedly contribute to magnetosheath fluctuations, their relatively low occurrence frequency suggests that they cannot explain a significant portion of the fluctuations that are continually present in the magnetosheath.

Shock Generation - Another source of fluctuations in the magnetosheath is undoubtedly the bow shock. A vast literature exists on collisionless shocks and their associated waves (e.g. Tidman and Krall, 1972; Biskamp, 1973) but a review of this topic is beyond the scope of this paper. Here we will review the very few studies that have concentrated on magnetosheath observations downstream of the bow shock.

Figure 17 shows the field magnitude and 3 solar ecliptic components across one of three bow shock crossings studied by Holzer et al., (1972). The high frequency ( 1.5 hz) waves in the low field upstream region are undoubtedly right hand polarized whistler mode waves propagating away from the shock and into the upstream region (Fairfield, 1974) and hence do not affect the magnetosheath. The lower frequency ( 0.3 hz) downstream waves were observed to be left hand elliptically polarized relative to the average field direction.

Furthermore, this polarization did not reverse when the shock motion reversed, thus demonstrating that the waves were not stationary in the shock frame of reference but rather were propagating with a velocity that is large compared to the shock-spacecraft velocity and presumably is in the downstream direction. The propagation vector of the downstream waves was not obviously related to the shock normal, the field direction or the plasma-flow velocity, but the major axis of the polarization ellipse was noted to be approximately aligned with the upstream propagation direction.

In the example in Figure 17 the angle between the upstream field and the shock normal was approximately  $60^\circ$ . This structure is probably typical of large angles; whereas, at smaller field-normal angles the bow shock degenerates into a much broader region of irregular pulsations (Greenstadt et al., 1970) and the (.01 - .05 hz) low frequency upstream waves are present. Under these latter conditions any distinction between shock generation versus upstream origin of the magnetosheath waves becomes extremely difficult, at least from the observational point of view.

Search coil experiments have also detected enhanced high frequency noise at the bow shock which may contribute to noise in the magnetosheath (Holzer et al., 1966).

Magnetopause Origin - Another possible source of magnetosheath fluctuations is the magnetopause. Many authors have discussed the possible Kelvin-Helmholtz instability of the magnetopause caused by the relative velocity between the magnetosheath and magnetosphere plasmas (e.g. Southwood, 1968; Boller and Stolov, 1973, and reference therein). In the most general analysis, Southwood (1968) has determined the nature of the wave modes that would be the first to go unstable if the magnetosheath velocity increased

from an initial low value. He finds that at low and middle magnetospheric latitudes these modes would exhibit circular polarization in a plane perpendicular to the magnetospheric field. Dungey and Southwood (1970)

checked these predictions using Explorer 33 data taken in the vicinity of the magnetopause. They found that waves with periods of the order of 10's of seconds had polarization which strongly supported the Kelvin Helmholtz instability theory. Although the primary interest of Dungey and Southwood was in waves inside the magnetosphere as an explanation of PC 2-5 micro-pulsations, they also noted that similar waves were seen on the magnetosheath side of the boundary where they contributed a substantial portion of the observed power.

Since high velocities as well as preferred field orientations create the conditions for the Kelvin Helmholtz instability, it is clear that instability is more likely along the downstream portion of the magnetopause where magnetosheath plasma velocities attain a larger fraction of their interplanetary values (see Figure 2). Boller and Stolov (1973) investigated IMP 1 magnetic field and plasma observations and, using a simplified instability criterion, concluded that indeed, the instability criteria were more often met in the downstream region. Wolfe and Kaufmann (1973) concluded that high magnetosphere to magnetosheath power density ratios occurred more frequently away from the earth-sun line and where Southwood's Kelvin Holmholtz stability criterion were met.

Even if the magnetopause is often Kelvin Helmholtz unstable over a significant magnetopause area, there remains the question of whether the waves can propagate rapidly enough relative to the magnetosheath plasma

that they will reach locations in the outer portion of the magnetosheath. On the basis of comparing typical propagation velocities with flow velocities (see Figures 2 and 14), it would seem that propagation to the remote regions of the magnetosheath is unlikely under most conditions.

For the example in Figures 11 and 12 we may take the measured magnetic field and the plasma values determined just before entry into the magnetosheath ( $n=6$ ,  $V=450$  km/sec) and supplied by the Los Alamos plasma experimenters. After scaling them according to Figure 2, we calculate a magnetosheath Alfvén velocity of 144 km/sec. This velocity is equal to three tenths of the solar wind velocity, showing that propagation from the magnetopause might be just marginally possible to explain the observations. Even if propagation to distant locations in the magnetosheath is not always possible, this source may have significant effect nearer the magnetopause and in the downstream magnetosheath.

#### Magnetosheath Generation

Generation of fluctuations within the magnetosheath is a relatively unexplored area. One suggestion for generating waves within the magnetosheath is that of Kaufmann et al., (1970) who suggested that the mirror instability might be responsible for the large amplitude .01 - .1 hz slow magnetoacoustic waves frequently observed. This instability, which occurs when  $p_{\perp} - p_{\parallel} > (p_{\parallel} / p_{\perp}) B^2 / 8\pi$ , causes plasma to become concentrated in regions of decreased field strength where it is confined by the high field "mirrors" of the adjacent regions. These plasma clouds, subsequently discussed by Kaufmann and Horng (1971), propagate slowly with the slow mode wave velocity.

Kovner and Feldstein (1973) suggest that when the component of

interplanetary field perpendicular to the earth-sun line is small, the magnetosheath plasma flow would be turbulent. Under these conditions diffusing plasma elements would stretch the frozen in magnetic field resulting in the spontaneous creation of large and irregular magnetic fields. (e.g. Ferraro and Plumpton, 1966). This suggestion has not been experimentally checked.

Two other proposals for generating magnetosheath waves are (1) an instability present when  $p_{\perp} > p_{\parallel}$  that generates transverse waves below the proton gyrofrequency (Noerdlinger, 1964) and (2) the cyclotron instability mentioned earlier as a means for producing 50-200 hz bursts in the magnetosheath.

#### IV. SUMMARY AND FUTURE WORK

The average magnetic field in the magnetosheath is relatively well understood. The magnetic field frozen in the solar wind plasma is convected into the magnetosheath by the streaming plasma. At the bow shock the field undergoes a compression and a minimal angle change necessary to preserve the normal component across the shock. Velocity differences within the magnetosheath lead to further distortion and an effective draping of the field over the magnetosphere, causing approximate tangency of the magnetosheath and magnetosphere fields. The typical high Alfvén mach number conditions of the solar wind allow a theoretical approximation which decouples the magnetohydrodynamic equations into a gas dynamic set and an electromagnetic set. The gas dynamic equations are first solved for the plasma parameters in the magnetosheath and the magnetic field is then calculated, assuming that the field is frozen in this plasma. Experimental results agree with theory to the accuracy of the comparison.

Future theoretical work will have to treat the full set of uncoupled equations, thus allowing the magnetic field to influence the plasma



parameters which in turn will change the magnetic field. Comparison of these higher order calculations with observations will be difficult, but is possible with high accuracy data. Comparisons under low mach number conditions when the field has its greatest influence should be most fruitful.

Time variation in the magnetosheath magnetic field are not as well understood as the average field. The simultaneous presence of many diverse and complicated wave modes of various frequencies make experimental study difficult. Fluctuations tend to be concentrated in the region below the proton gyrofrequency and power spectra in this low frequency region often contain peaks. On the average, such spectra show a decrease with increasing frequency which is roughly proportional to  $1/f$  or  $1/f^2$ . Above the proton gyrofrequency, the power spectrum decrease approximately as  $1/f^3$ . At the lowest frequencies, transverse waves tend to dominate, but slow magnetosonic mode waves are usually more prevalent in the .01 to .1 hz range. Wave perturbation vectors tend to align themselves with the shock or magnetopause surfaces.

Magnetosheath waves probably originate in a variety of ways but the relative importance of various sources is not clear. Upstream waves convected through the bow shock are undoubtedly an important source of waves, at least at certain times and in certain locations. Additional waves are surely generated at the bow shock, but the relative importance of this source is not known. Instabilities within the magnetosheath may generate waves, but neither theory nor experiment has investigated this possibility to any great extent. The magnetopause is another possible wave source, although such waves probably could not propagate to all regions of the magnetosheath from this location.

Experimental work will have to take the lead in future investigations of fluctuations. Such studies should attempt to isolate individual wave modes using filtering and modern methods for determining propagation directions. Comparison of simultaneous data from several experiments is a very important and relatively unexploited technique for determining wave modes and studying instability criteria.

The study of the magnetosheath has the potential for yielding much insight into instabilities and wave particle interactions which influence the behavior of tenuous collisionless plasmas. Understanding this behavior should contribute both to pure plasma physics and to a further understanding of the interaction of the solar wind with the geomagnetic field, and with other bodies in the solar system.

ACKNOWLEDGEMENTS

The author gratefully acknowledges the support of Dr. N. F. Ness, who is principle investigator for the IMP experiments, and Mr. J. B. Seek, J. L. Scheifele, and C. S. Scarce who carried out the engineering aspects of the experiments.

**PRECEDING PAGE BLANK NOT FILMED**

## References

- Alksne, Alberta Y., The Steady-State Magnetic Field in the Transition Region Between the Magnetosphere and the Bow Shock, Planet. Space Sci., 15, 239-245, 1967.
- Alksne, Alberta Y., and David L. Webster, Magnetic and Electric Fields in the Magnetosheath, Planet Space Sci., 18, 1203-1212, 1970.
- Asséo, E., and G. Berthomieu, Amplification of Hydromagnetic Waves Through the Earth's Bow Shock, Planet. Space Sci., 18, 1143-1152, 1970.
- Auer, Rolf-Dieter, Magnetohydrodynamic Aspects of the Earth's Bow Shock, 1, Equilibrium Bow Shock Position, J. Geophys. Res., 79, 5118-5120, 1974.
- Barnes, A., Collisionless Damping of Hydromagnetic Waves, Phys. Fluids, 9, 1483-1495, 1966.
- Barnes, A., Theory of Generation of Bow-Shock-Associated Hydromagnetic Waves in the Upstream Interplanetary Medium, Cosmic Electrodynamics, 1, 90-114, 1970.
- Behannon, K. W., and D. H. Fairfield, Spatial Variations of the Magnetosheath Magnetic Field, Planet. Space Sci., 17, 1803-1816, 1969.
- Biskamp, D., Collisionless Shock Waves in Plasmas, Nucl. Fusion, 13, 719-740, 1973.
- Blackman, R. B., and J. W. Tukey, The Measurement of Power Spectra, Dover Publications Inc. New York, 1958.
- Boller, B. R., and H. L. Stolov, Explorer 18 Study of the Stability of the Magnetopause using a Kelvin-Helmholtz instability criterion, J. Geophys. Res., 78, 8078-8086, 1973.
- Burlaga, L. F., Microstructure of the Interplanetary Medium, in Solar Wind,

- the Asilomar Conference Proceedings edited by C. P. Sonett,  
P. J. Coleman, Jr., and J. M. Wilcox, Superintendent of Documents,  
U. S. Government Printing Office, Washington, D.C., p.309-332, 1972.
- Burlaga, L. F., and N. F. Ness, Tangential Discontinuities in the Solar  
Wind, *Solar Physics*, 9, 467-477, 1969.
- Cahill, L. J., and P. G. Amazeen, The Boundary of the Geomagnetic Field,  
*J. Geophys. Res.*, 68, 1835-1843, 1963.
- Coleman, P. J., Jr., Characteristics of the Region of Interaction Between  
the Interplanetary Plasma and the Geomagnetic Field: Pioneer 5,  
*J. Geophys. Res.*, 69, 3051-3076, 1964.
- Coleman, P. J. Jr., Variations in the Interplanetary Magnetic Field:  
Mariner 2, 1, Observed Properties, *J. Geophys. Res.*, 71, 5509-5531,  
1966.
- Cummings, W. D., and P. J. Coleman, Jr., Magnetic Fields in the Magnetopause  
and Vicinity at Synchronous Altitude, *J. Geophys. Res.*, 73, 5699-5718, 1968.
- Dryer, M., and R. Faye-Petersen, Magnetogasdynamic Boundary Condition  
for a Self Consistent Solution to the Closed Magnetopause, *AIAA J.*,  
4, 246-254, 1966.
- Dryer, M., and G. R. Heckman, On the Hypersonic Analogue as Applied to  
Planetary Interaction with the Solar Plasma, *Planet. Space Sci.*, 15,  
515-546, 1967.
- Dryer, M., Solar Wind Interactions-Hypersonic analogue, *Cosmic Electro-  
dynamics*, 1, 115-142, 1970.
- Dungey, J. W., and D. J. Southwood, Ultra Low Frequency Waves in the  
Magnetosphere, *Space Science Reviews*, 10, 672-688, 1970.
- Fairfield, D. H., The Ordered Magnetic Field of the Magnetosheath, *J. Geophys.  
Res.*, 72, 5865-5877, 1967.

- Fairfield, D. H., Simultaneous Measurements on Three Satellites and the Observation of the Geomagnetic Tail at  $1000 R_E$ , J. Geophys. Res., 73, 6179-6187, 1968.
- Fairfield, D. H., Bow Shock Associated Waves Observed in the Far Upstream Interplanetary Medium, J. Geophys. Res., 74, 3541-3553, 1969.
- Fairfield, D. H., Average and Unusual Locations of the Earth's Magnetopause and Bow Shock, J. Geophys. Res., 76, 6700-6716, 1971.
- Fairfield, D. H., Whistler Waves Observed Upstream from Collisionless Shocks, J. Geophys. Res., 79, 1368-1378, 1974.
- Fairfield, D. H., and N. F. Ness, Magnetic Field Fluctuations in the Earth's Magnetosheath, J. Geophys. Res., 75, 6050-6060, 1970.
- Fairfield, D. H., and N. F. Ness, IMP 5 Magnetic Field Measurements in the High Latitude Outer Magnetosphere Near the Noon Meridian, J. Geophys. Res., 77, 611-623, 1972.
- Ferraro, V.C.A., and C. Plumpton, An Introduction to Magneto-fluid Mechanics, Oxford University Press, London, second edition, 1966.
- Formisano, V., P. C. Hedgecock, G. Moreno, J. Sear, and D. Bollea, Observations of Earth's Bow Shock for Low Mach Numbers, Planet. Space Sci., 19, 1519-1531, 1971.
- Formisano, V., G. Moreno, F. Palmiotto, and P. C. Hedgecock, Solar Wind Interaction with the Earth's Magnetic Field, 1, Magnetosheath, J. Geophys. Res., 78, 3714-3730, 1973.
- Greenstadt, E. W., G. T. Inouye, I. M. Green, and D. L. Judge, Vela 3 Magnetograms at  $18 R_E$  Structure and Pulsations in the Magnetosheath, J. Geophys. Res., 72, 3855-3876, 1967.
- Greenstadt, E. W., Binary Index for Assessing Local Bow Shock Obliquity, J. Geophys. Res., 72, 5467-5479, 1972.

- Ness, N. F., Clell S. Scarce, and J. B. Seek, Initial Results of the IMP 1 Magnetic Field Experiment, J. Geophys. Res., 69, 3531-3569, 1964.
- Ness, N. F., C. S. Scarce and S. Cantarano, Preliminary Results from the Pioneer 6 Magnetic Field Experiment, J. Geophys. Res., 71, 3305-3313, 1966.
- Neubauer, F. M., Nonlinear Interaction of a Fast Magnetogasdynamical Shock with a Tangential Discontinuity, preprint, Institut für Geophysik und Meteorologie, Braunschweig, 1973.
- Neubauer, F. M., Nonlinear Oblique Interaction of Interplanetary Discontinuities with the magnetogasdynamical Bow Shock, submitted to J. Geophys. Res., 1974.
- Noerdlinger, P. D., Wave Generation Near the Outer Boundary of the Magnetosphere, J. Geophys. Res., 69, 369-375, 1964.
- Olson, J. V., R. E. Holzer, and E. J. Smith, High Frequency Magnetic Fluctuations Associated with the Earth's Bow Shock, J. Geophys. Res., 74, 4601-4617, 1969.
- Rigby, B. J., and J. S. Mainstone, The Effect of the Earth's Bow Shock and Magnetosheath on the Interaction of a Discontinuity in the Solar Wind with the Magnetosphere, Planet. Space Sci., 21, 499-506, 1973.
- Scarf, F. L., R. W. Fredricks, M. Neugebauer and C. T. Russell, Plasma Waves in the Dayside Polar Cusp 2. Magnetopause and Polar Magnetosheath. J. Geophys. Res., 79, 511-520, 1974.
- Schatten, K. H., Large-scale Properties of the Interplanetary Magnetic Field, in Solar Wind, edited by C. P. Sonett, P. J. Coleman Jr., and J. M. Wilcox, U. S. Government Printing Office, Washington, D. C., p. 65-92, 1972.
- Shen, Wen-Wu, The Earth's Bow Shock in an Oblique Interplanetary Field, Cosmic Electrodynamics, 2, 381-395, 1972.

- Siscoe, G. L., L. Davis, Jr., E. J. Smith, P. J. Coleman, Jr., and  
D. E. Jones, Magnetic Fluctuations in the Magnetosheath: Mariner 4,  
J. Geophys. Res., 72, 1-17, 1967a.
- Siscoe, G. L., L. Davis, Jr., P. J. Coleman, Jr., E. J. Smith, and  
D. E. Jones, Shock Aligned Magnetic Oscillations in the Magnetosheath:  
Mariner 4, J. Geophys. Res., 72, 5524-5530, 1967b.
- Siscoe, G. L., L. Davis, Jr., P. J. Coleman, Jr., E. J. Smith, and  
D. E. Jones, Power Spectra and Discontinuities of the Interplanetary  
Magnetic Field, J. Geophys. Res., 73, 61-82, 1968.
- Smith, E. J., R. E. Holzer, M. G. McLeod, and C. T. Russell, Magnetic Noise  
in the Magnetosheath in the Frequency Range 3-300 Hz, J. Geophys. Res.,  
72, 4803-4813, 1967.
- Smith, E. J., R. E. Holzer, and C. T. Russell, Magnetic Emissions in the  
Magnetosheath at Frequencies Near 100 Hz., J. Geophys. Res., 74,  
3027-3036, 1969.
- Smith, E. J., and L. Davis, Jr., Magnetic Measurements in the Earth's  
Magnetosphere and Magnetosheath: Mariner 5, J. Geophys. Res., 75,  
1233-1245, 1970.
- Sonett, C. P., The Distant Geomagnetic Field 4. Microstructure of a  
Disordered Hydromagnetic Medium in the Collisionless Limit, J. Geophys.  
Res., 68, 1265-1294, 1963.
- Sonett, C. P., A. R. Sims, and E. J. Smith, Rocket Surveys of the Distant  
Geomagnetic Field in Space Research, 921-937, edited by H. J. K llmann-Bijl,  
North Holland Publishing Co., Amsterdam, 1960.
- Sonett, C. P., D. L. Judge, and J. M. Kelso, Evidence Concerning Instabilities  
of the distant Geomagnetic Field: Pioneer 1, J. Geophys. Res., 64,  
941-943, 1959.



- Sonett, C. P., and I. J. Abrams, The Distant Geomagnetic Field, 3, Disorder and Shocks in the Magnetopause, J. Geophys. Res., 68, 1233-1263, 1963.
- Sonnerup, B.U.O., and L. J. Cahill, Jr., Magnetopause Structure and Attitude from Explorer 12 Observations, J. Geophys. Res., 72, 171-183, 1967.
- Southwood, D. J., The Hydromagnetic Stability of the Magnetospheric Boundary, Planet. Space Sci., 16, 587-605, 1968.
- Spreiter, J. R., A. L. Summers, and A. Y. Alksne, Hydromagnetic Flow Around the Magnetosphere, Planet. Space Sci., 14, 223-253, 1966a.
- Spreiter, J. R., A. L. Summers, and A. Y. Alksne, A Fluid Model for the Interaction of the Solar Wind and the Geomagnetic Field, in Radiation Trapped in the Earth's Magnetic Field, Edited by Billy McCormac, D. Reidel Pub. Co., Dordrecht, Holland, 1966b.
- Spreiter, J. R., A. Y. Alksne, and A. L. Summers, External Aerodynamics of the Magnetosphere, in Physics of the Magnetosphere, edited by R. L. Carovillano, J. F. McClay and H. R. Radoski, D. Reidel Pub. Co., Dordrecht, Holland, 301-375, 1968.
- Spreiter, J. R., and A. Y. Alksne, Plasma Flow Around the Magnetosphere, Rev. Geophys. Space Phys., 7, 11-50, 1969.
- Svalgaard, Lief, The Relation Between the Azimuthal Component of the Interplanetary Magnetic Field and the Geomagnetic Field in the Polar Caps, in Correlated Interplanetary and Magnetospheric Observations edited by D. E. Page, D. Reidel Pub. Co., Dordrecht, Holland, 1974.
- Tidman, D. A., and N. A. Krall, Shock Waves in Collisionless Plasmas, Wiley-Interscience, New York, 1972.
- Volk, H. J., and R. D. Auer, Motions of the Bow Shock Induced by Interplanetary Disturbances, J. Geophys. Res., 79, 40-48, 1974.
- Walters, G. K., Effect of Oblique Interplanetary Magnetic Field on Shape and Behavior of the Magnetosphere, J. Geophys. Res., 69, 1769-1783, 1964.

Walters, G. K., On the Existence of a Second Standing Shock Wave Attached to the Magnetosphere, J. Geophys. Res., 71, 1341-1344, 1966.

Westphal, K. O., and J. F. McKenzie, Interaction of Magnetoacoustic and Entropy Waves with Normal Magnetohydrodynamic Shock Waves, Physics Fluids, 12, 1228-1236, 1969.

Wolfe, A., and R. L. Kaufmann, MHD Wave Transmission and Production Near the Magnetopause, preprint 1973.

Wolfe, J. H., and D. S. Intriligator, The Solar Wind Interaction with the Geomagnetic Field, Space Science Rev., 10, 511-596, 1970.

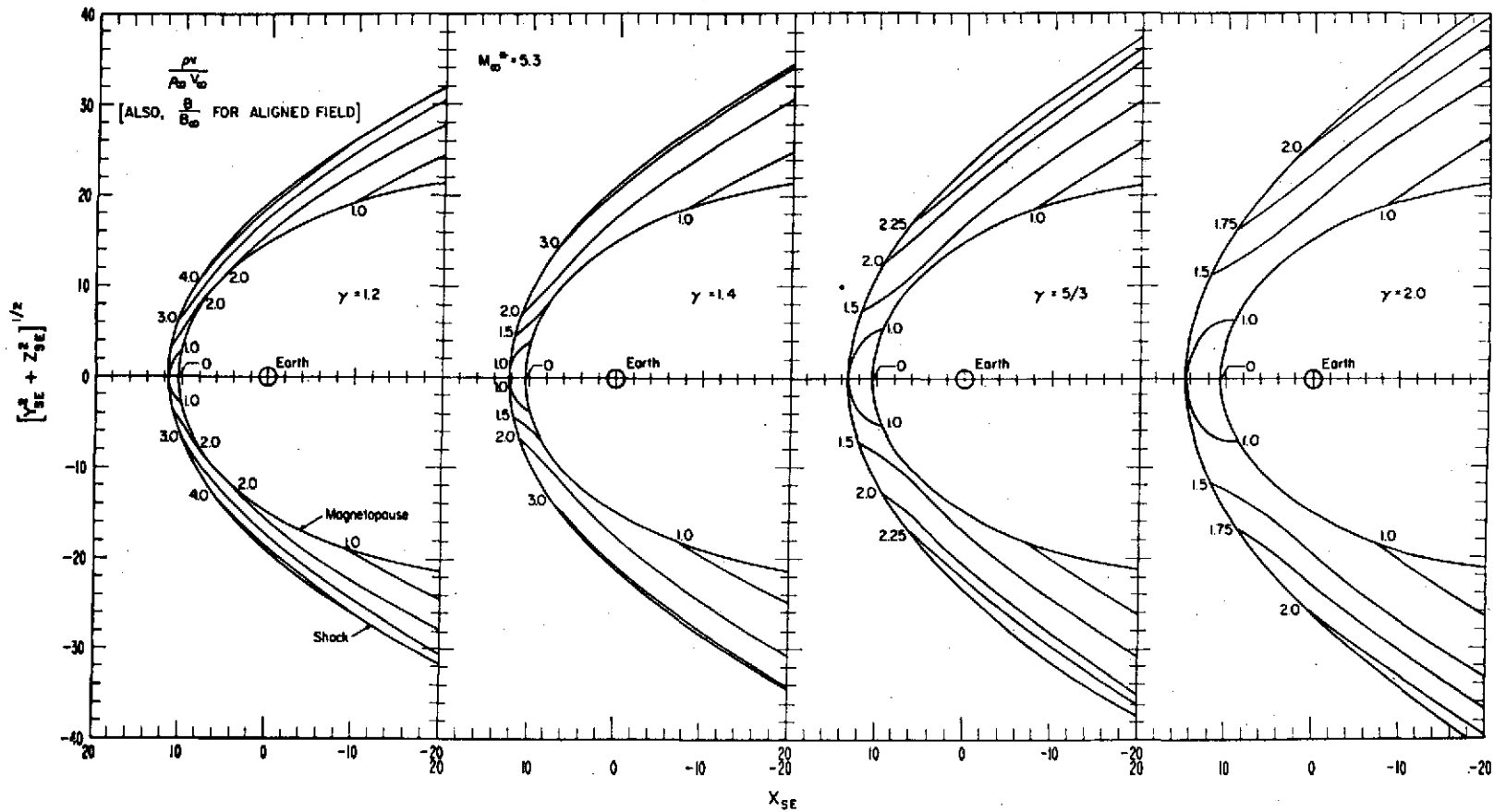
## FIGURE CAPTIONS

- Figure 1       Contours of normalized magnetic field strength in the magnetosheath for four values of specific heat ratio  $\gamma$ .  
(Dryer, 1972)
- Figure 2       Contours of normalized plasma parameters in the magnetosheath. Upstream gas dynamic mach number is 8.71 and specific heat ratio is 2. (Spreiter et al., 1966b)
- Figure 3       Magnetic field configuration and intensity in two planes. The upstream field lines are in a plane parallel to the plane of symmetry through the center of the earth, but offset from it by a distance equal to 1/3 the distance to the stagnation point. (Spreiter et al., 1968)
- Figure 4       Simultaneous magnetosheath and interplanetary magnetic field measurements from Explorers 33 and 34.
- Figure 5       Projections of IMP 2 magnetosheath vectors in the XY plane are shown for 4 different directional groupings of the interplanetary field. For  $0^\circ < \phi < 180^\circ$  the magnetosheath fields tend to point toward dusk, and for  $180^\circ < \phi < 360^\circ$  the fields point toward dawn.
- Figure 6       Comparison between experimental values of the normalized magnetosheath field magnitude and theoretical contours, for the case of the interplanetary field oriented transverse to the earth-sun line.
- Figure 7       Averages of normalized magnetosheath magnetic field magnitude for intervals of  $10 R_E$  along the earth-sun line showing the continuous decrease of the magnetosheath field with distance downstream.

- Figure 8 XY plane projection of magnetosheath field vectors for cases when the interplanetary field was oriented at  $30^{\circ}$ - $40^{\circ}$  from the earth-sun line.
- Figure 9 Composite of magnetosheath magnetic field magnitude spectra covering 11 decades in power and more than 4 decades in frequency.
- Figure 10 Relative power in the two components transverse to the average field versus the angle the X axis makes with a theoretical shock normal. When the angle is small and X is aligned near the shock normal, there is considerably more power in the Y component which tends to be aligned with the shock surface.
- Figure 11 A representative data interval illustrating waves in the field magnitude on a magnetosheath pass near the earth-sun line when the interplanetary field was oriented transverse to the earth-sun line. The Z axis is aligned with the normal to a model magnetopause.
- Figure 12 Power spectra of the field magnitude and the field components perpendicular to the average field direction computed from simultaneous measurements in the magnetosheath and in the interplanetary medium. There is no interplanetary enhancement corresponding to the magnetosheath peak near .06 hz. The data interval includes that of Figure 11.
- Figure 13 Data from 5 OGO-3 spectrum analyzer channels on a representative inbound pass. Broadband, time-varying noise is seen throughout the magnetosheath between 10 and 800 hz. (Smith et al., 1969)

- Figure 14 Phase velocity as a function of frequency for propagation along and perpendicular to the magnetic field. Horizontal dashed lines denote the typical range of plasma flow velocities.
- Figure 15 Simultaneous data from two spacecraft in the vicinity of the bow shock.
- Figure 16 Twenty second standard deviations averaged over many magnetosheath passes and plotted versus orbit number or (equivalently) solar ecliptic longitude.
- Figure 17 OGO-5 data in solar ecliptic coordinates illustrating 0.3 hz waves immediately downstream from the bow shock. (Holzer et al., 1972)

Figure 1



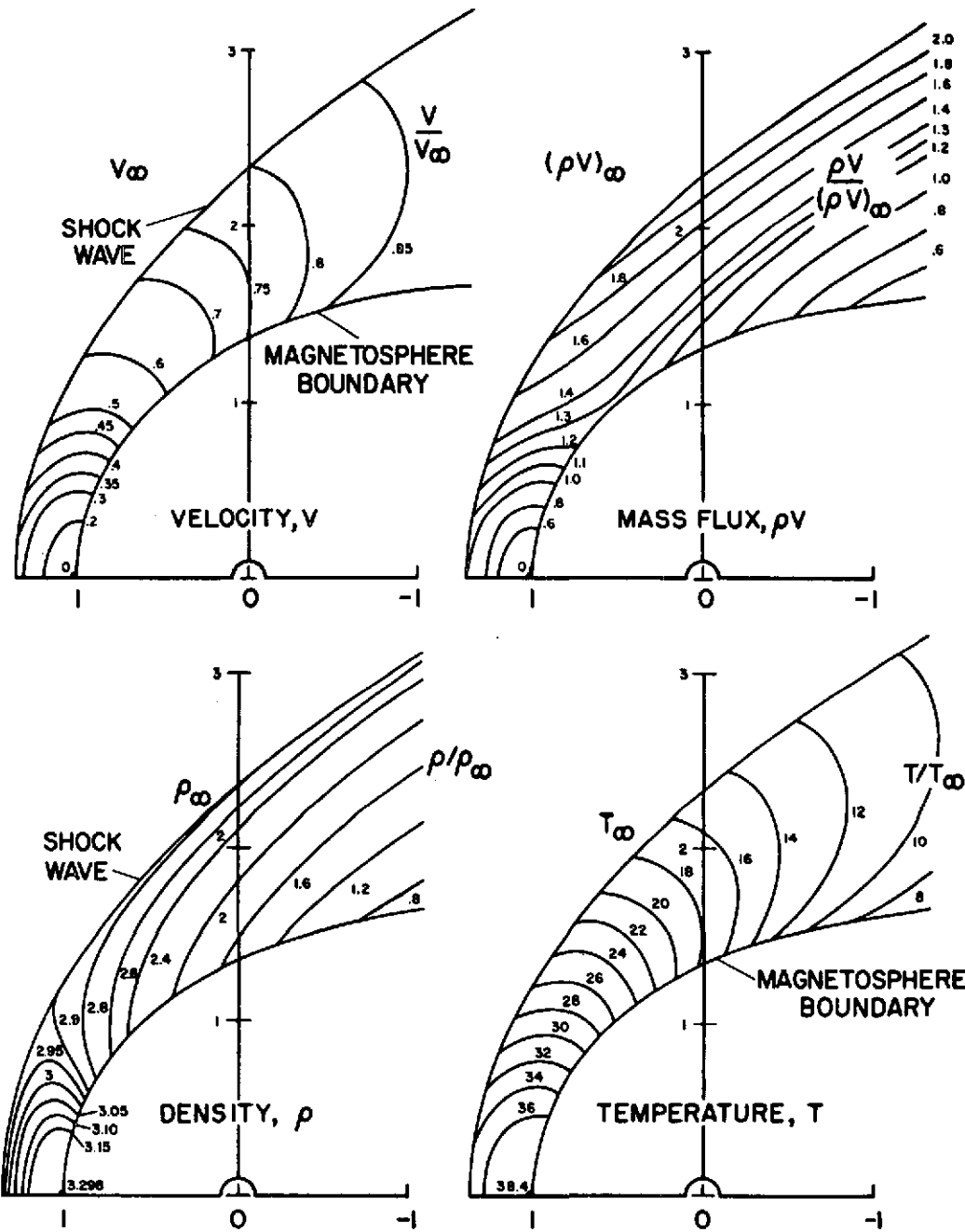


Figure 2

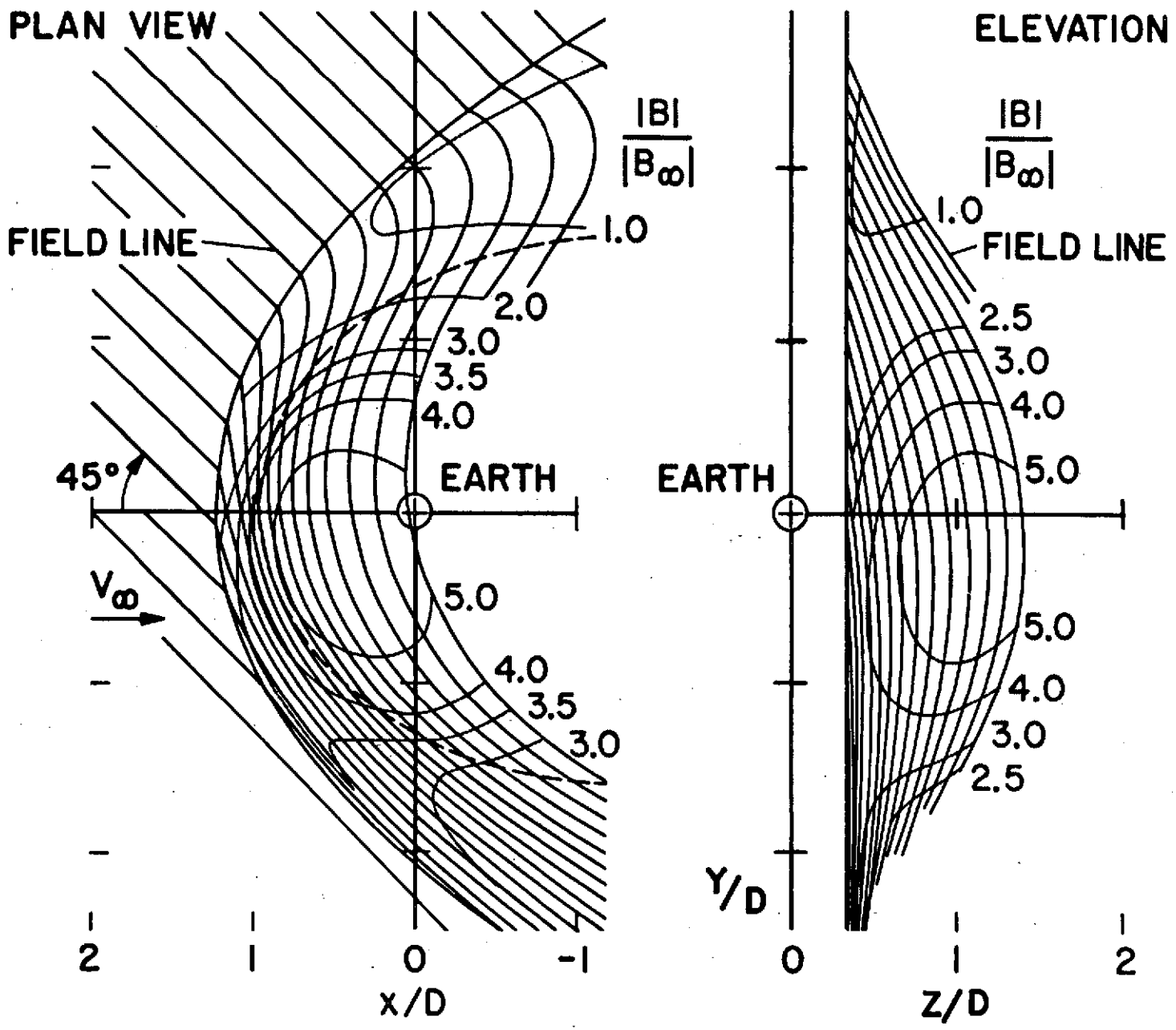


Figure 3



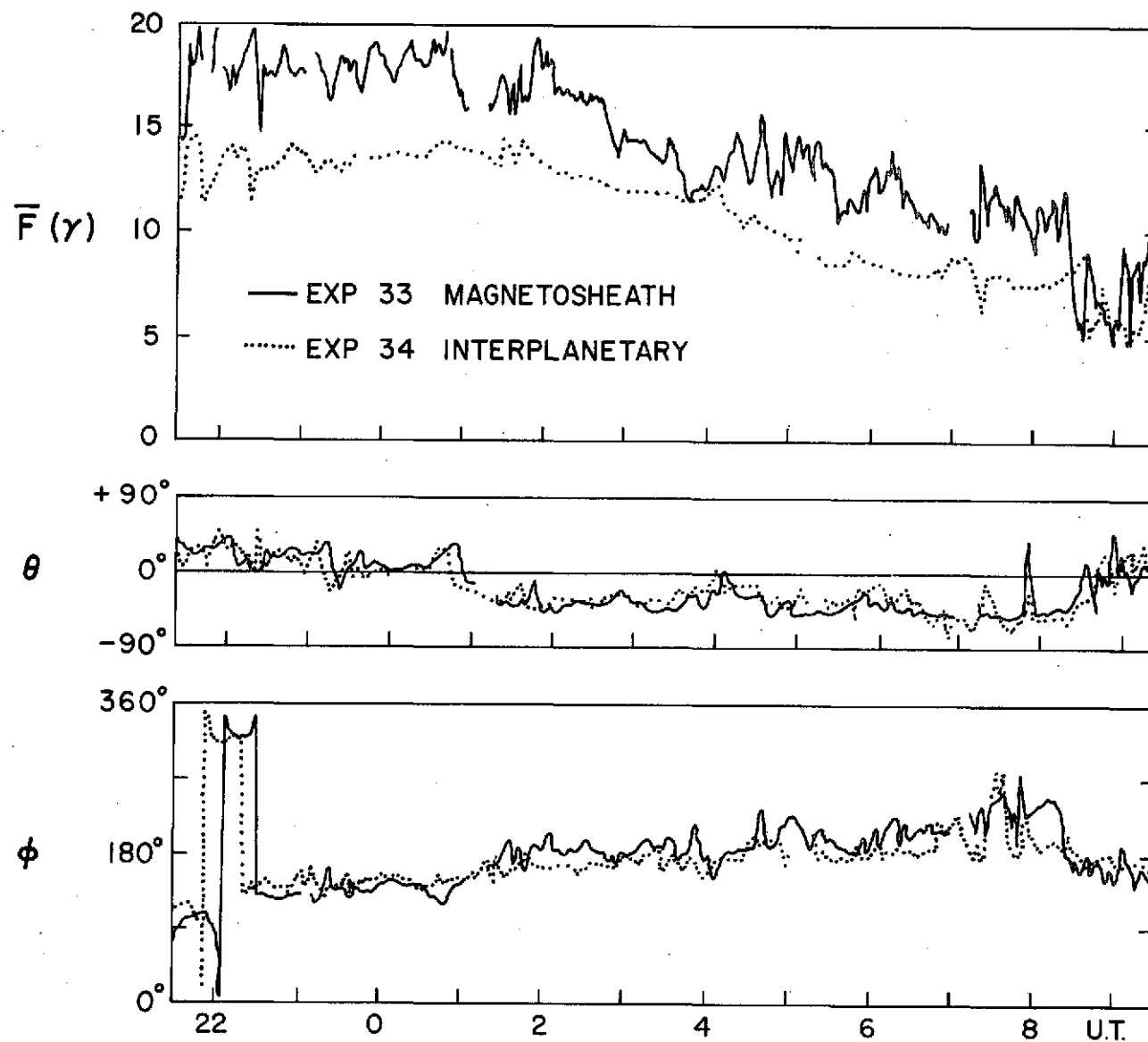


Figure 4

SEPTEMBER 20-21, 1967

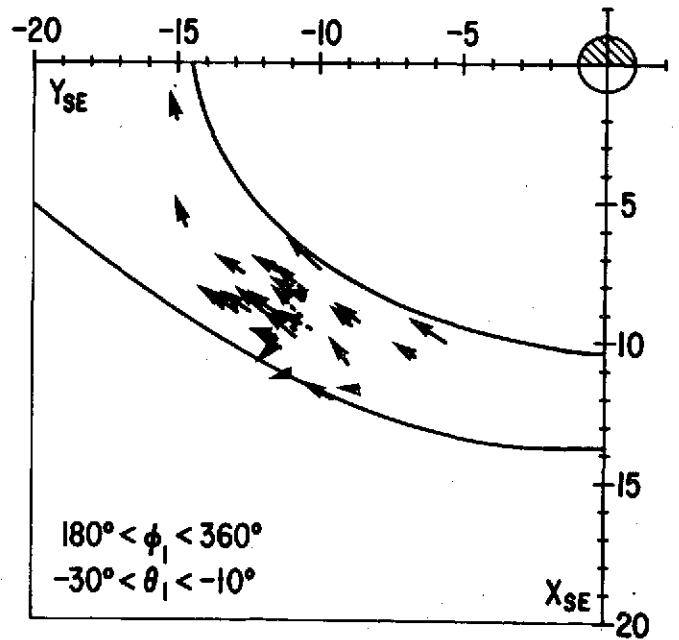
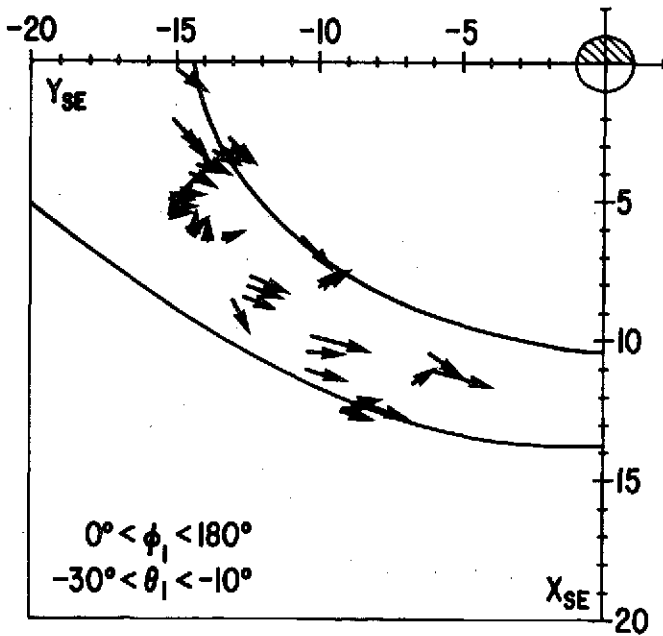
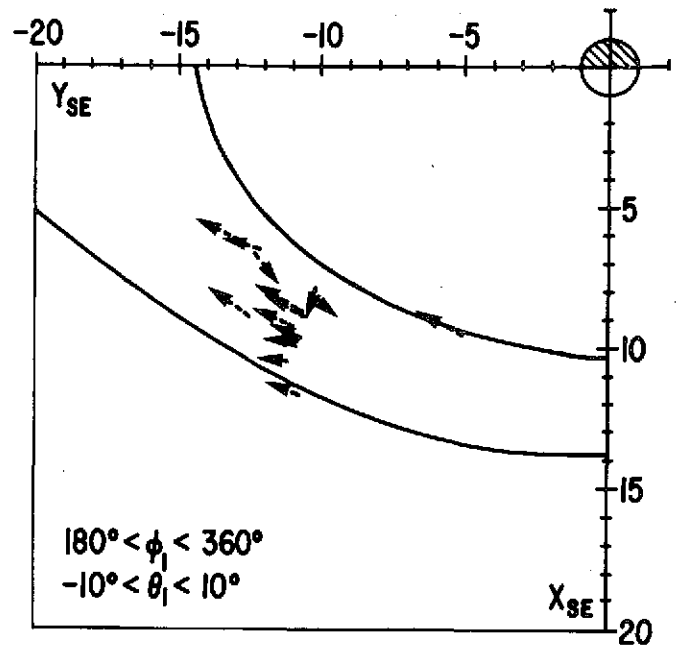
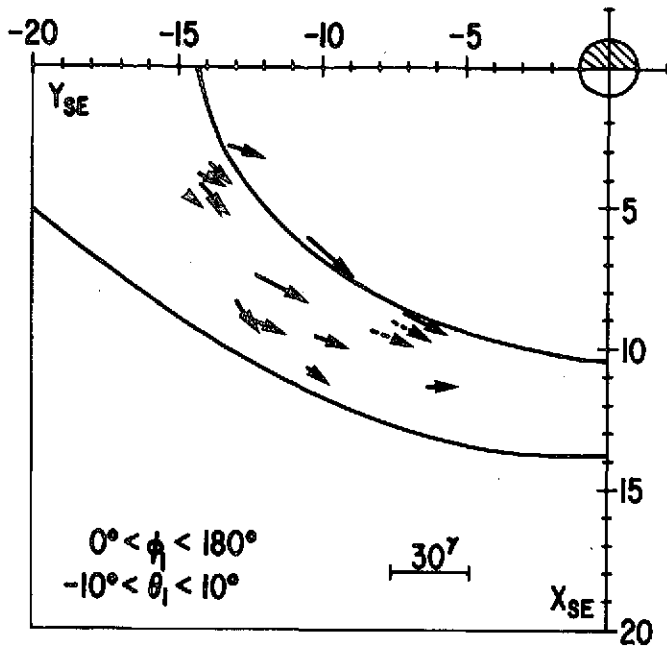


Figure 5

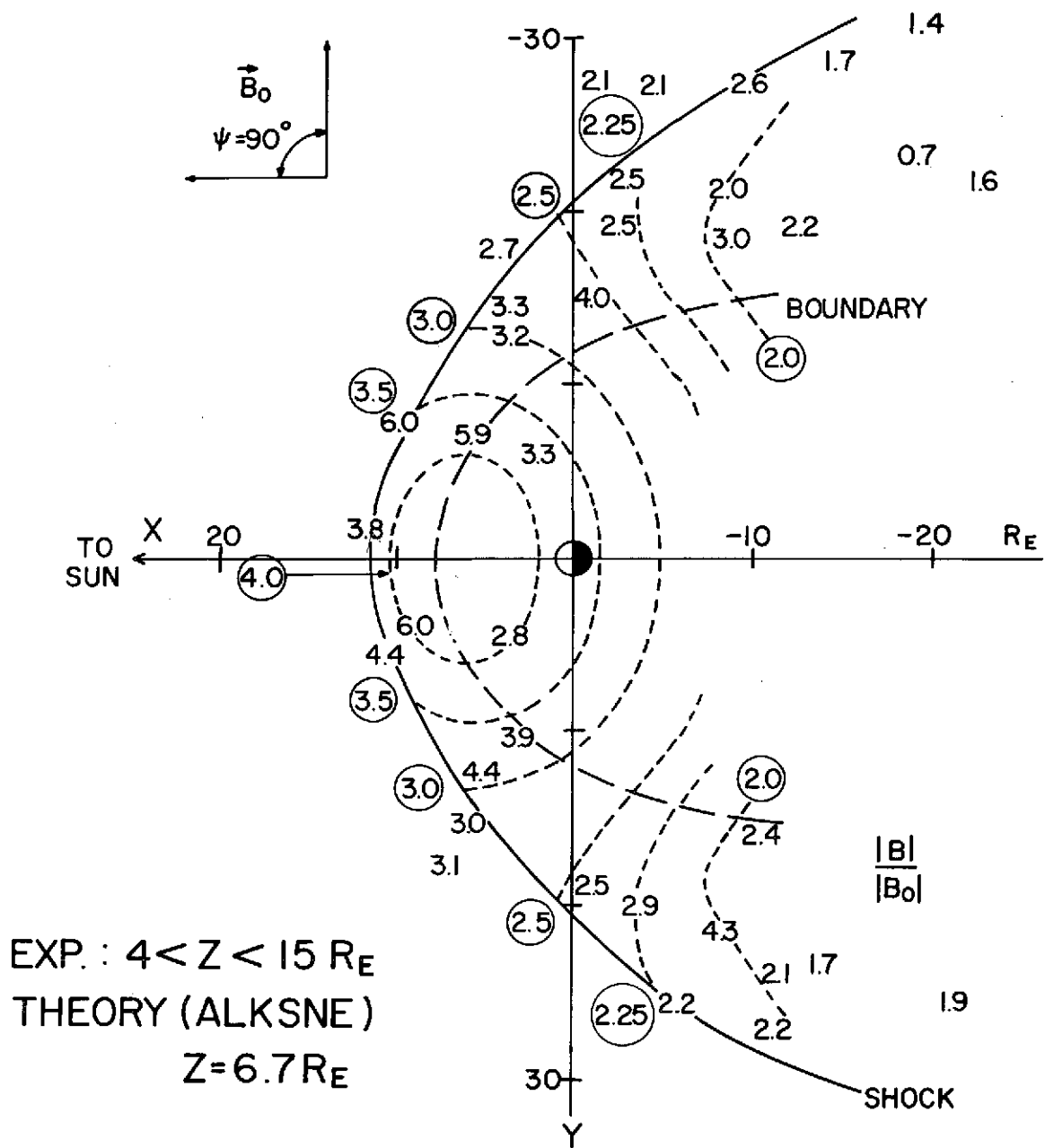


Figure 6

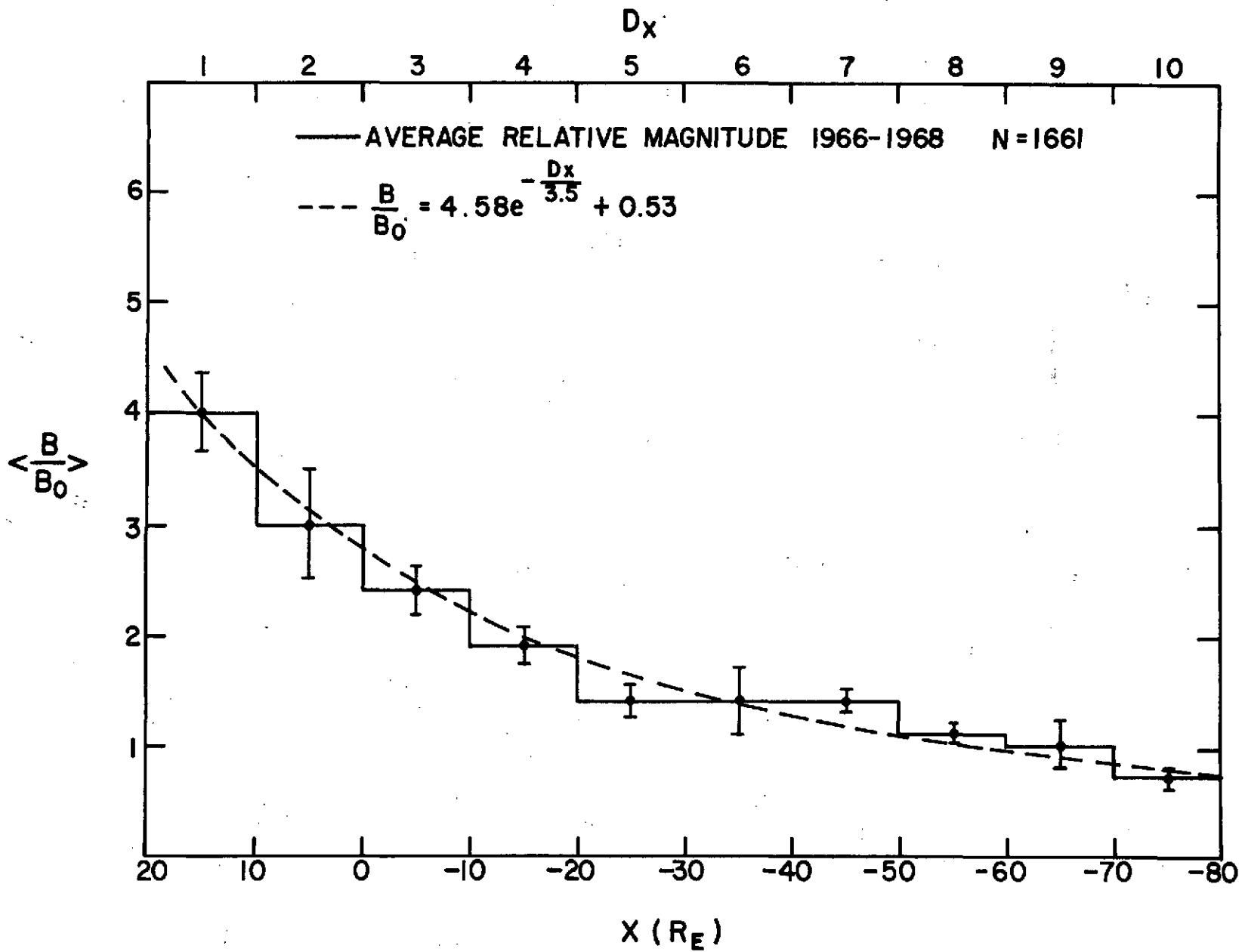


Figure 7

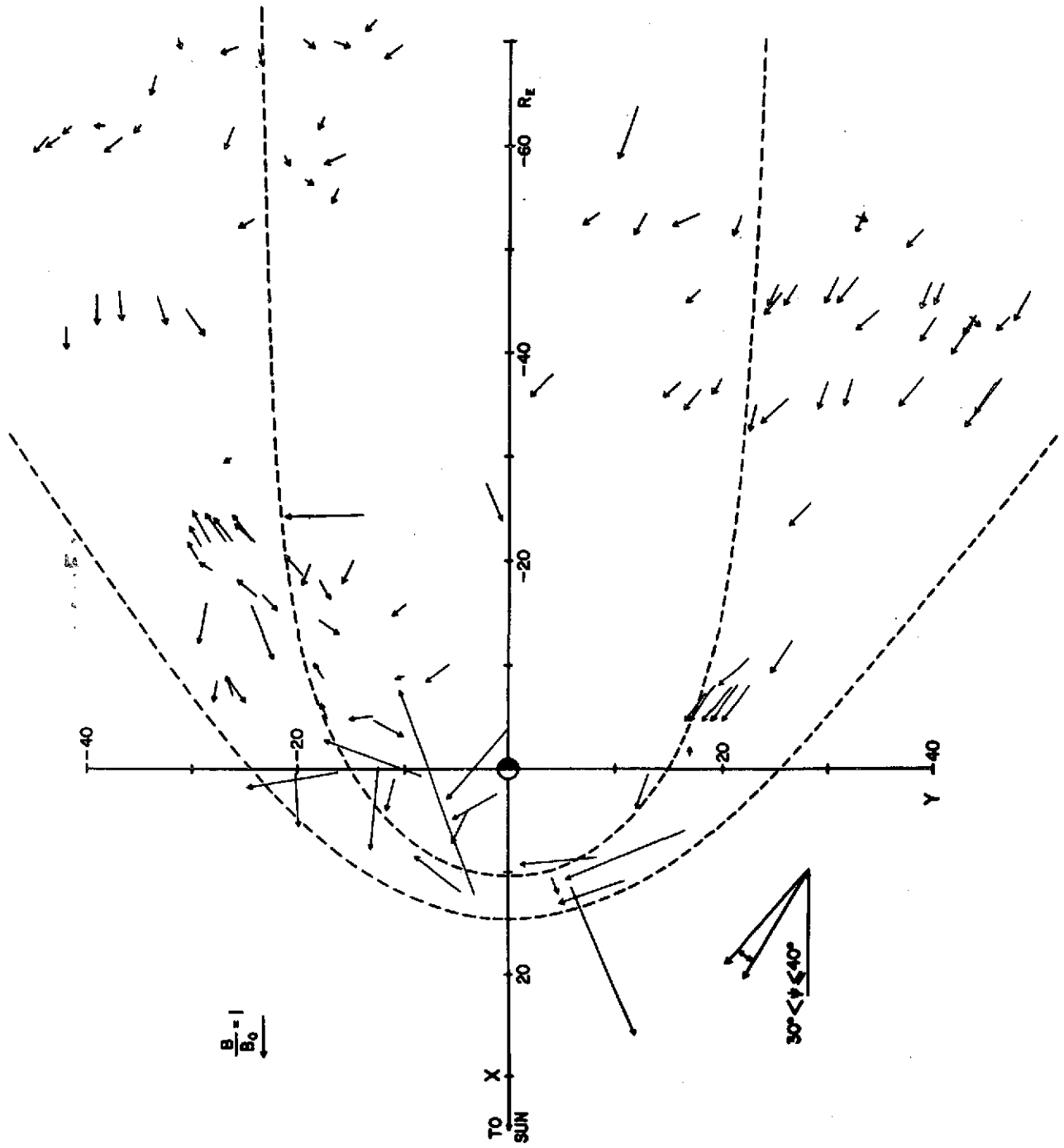


Figure 8

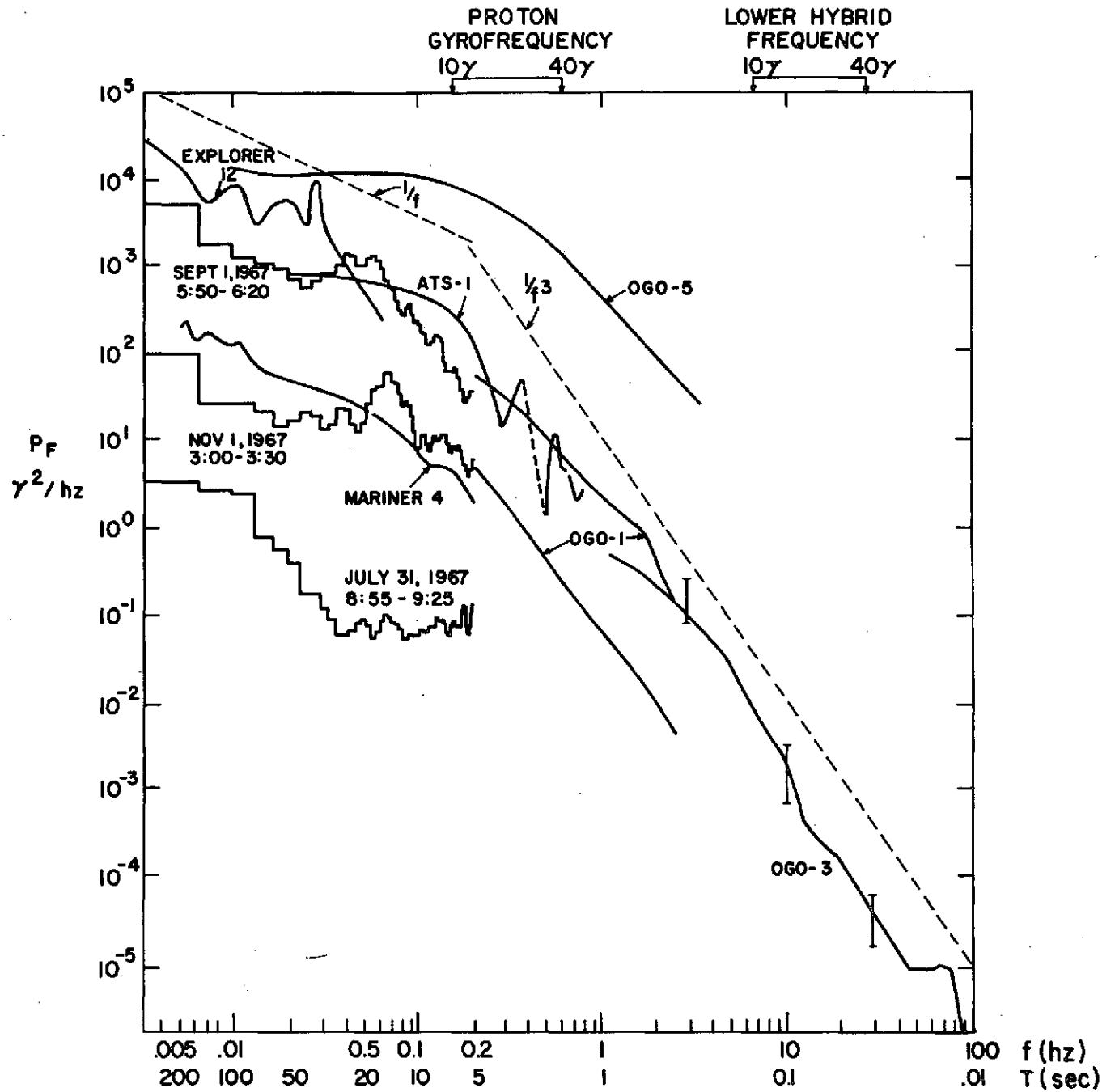


Figure 9

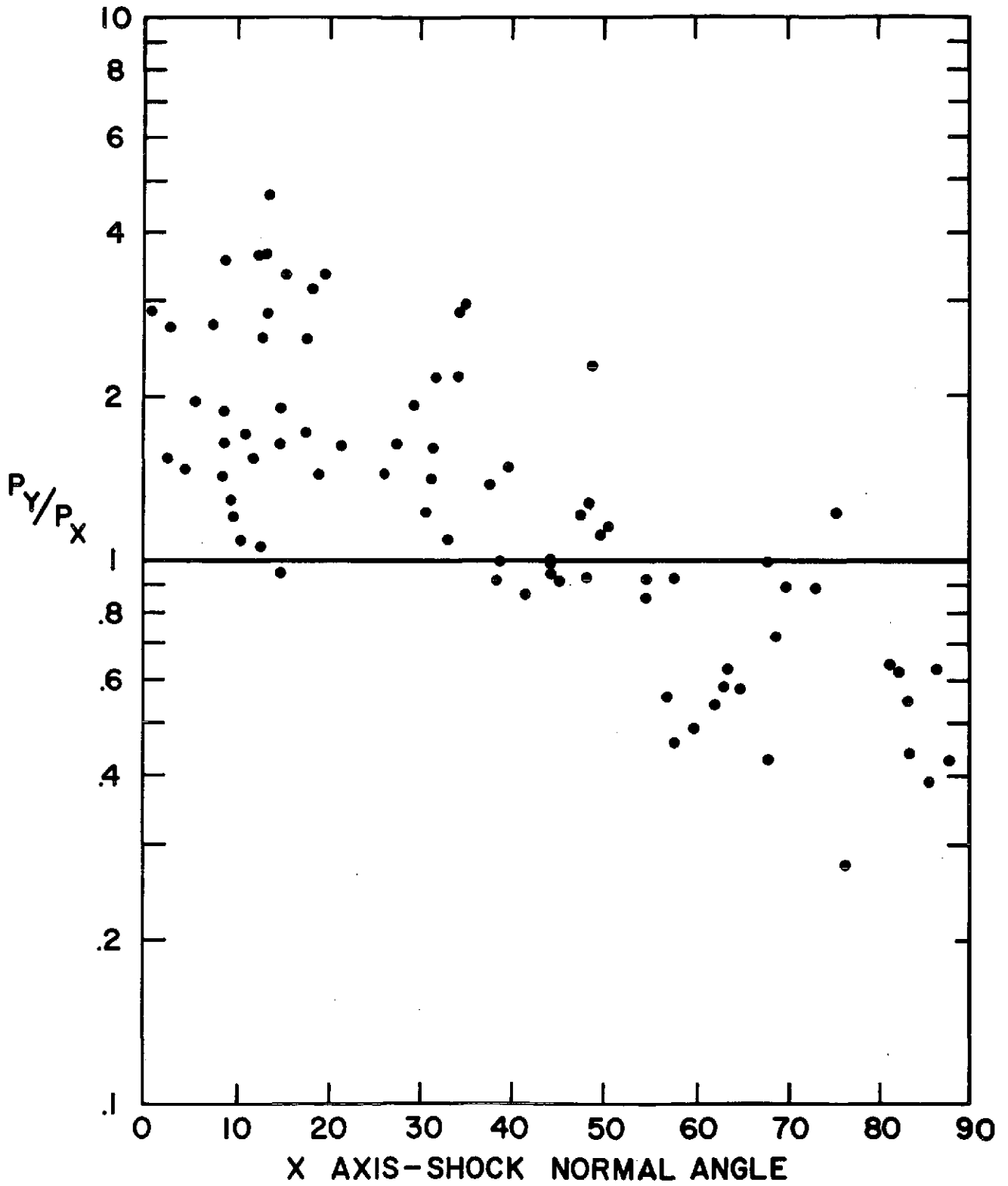


Figure 10

Figure 11

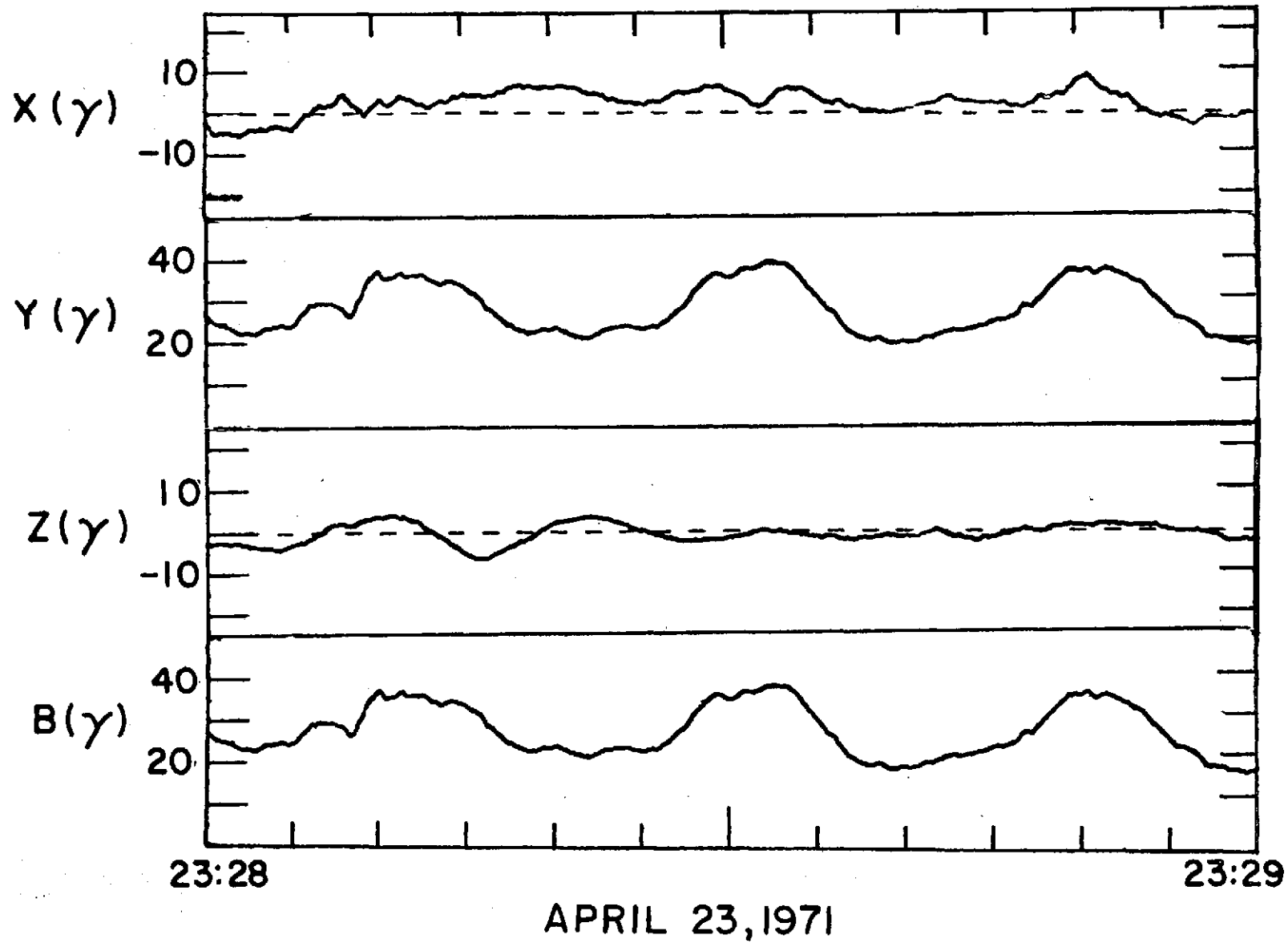
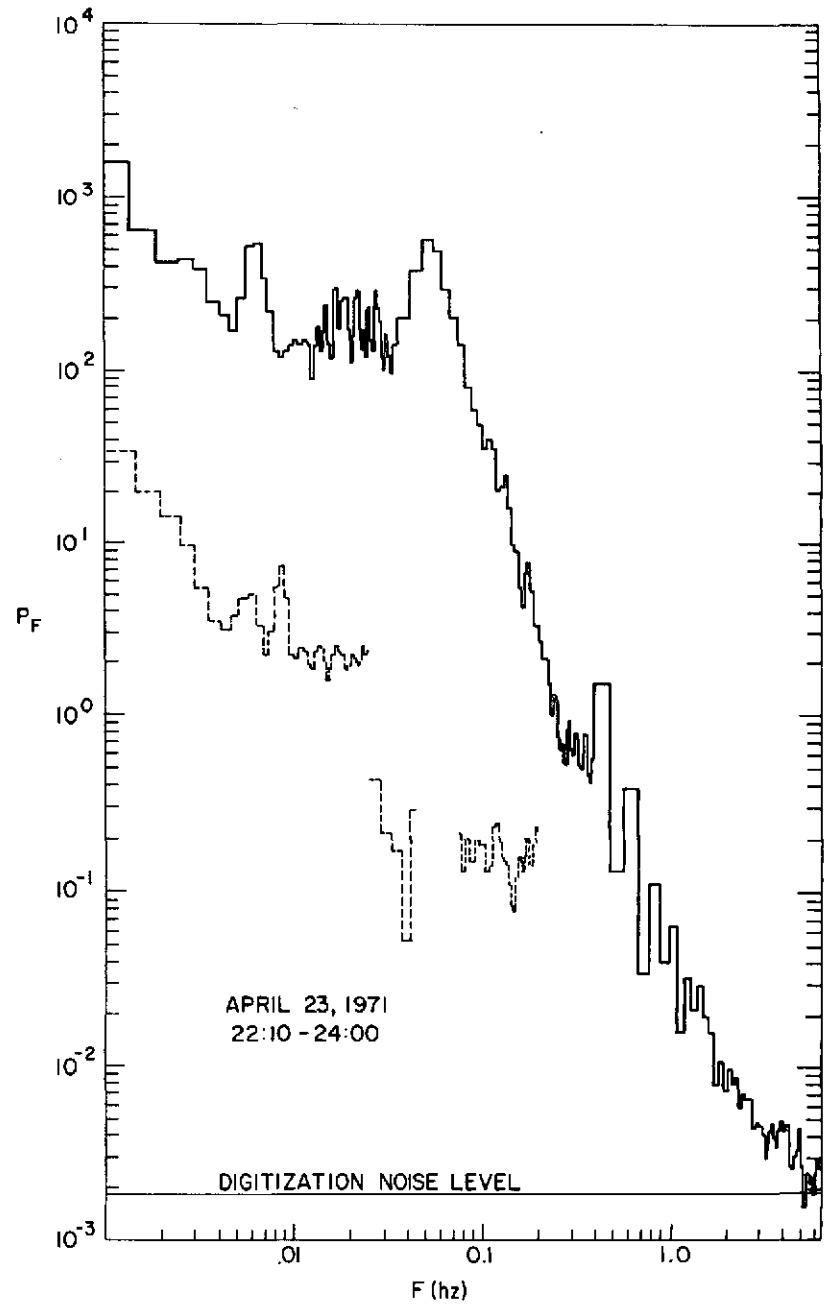
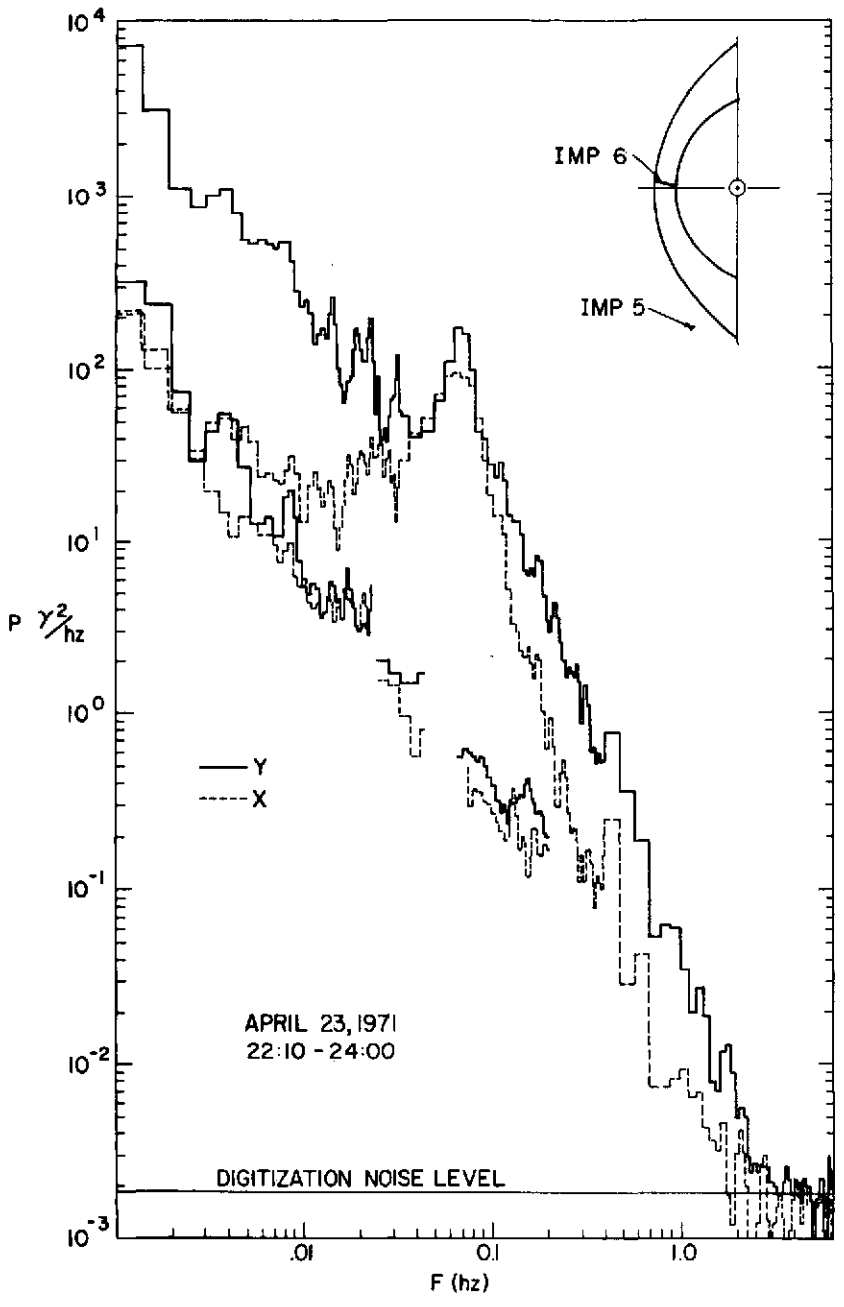


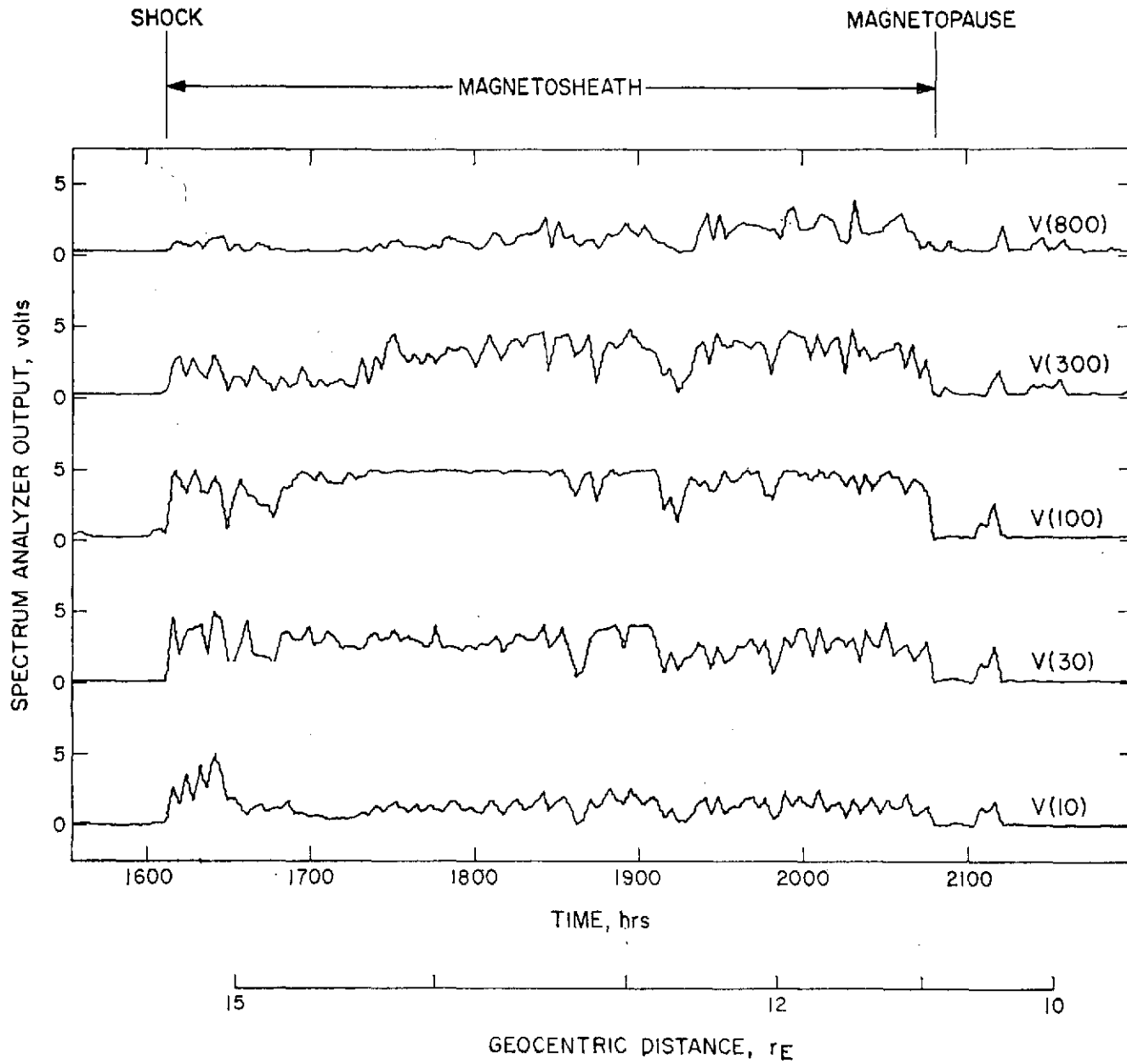


Figure 12



ORIGINAL PAGE IS  
OF POOR QUALITY

Figure 13



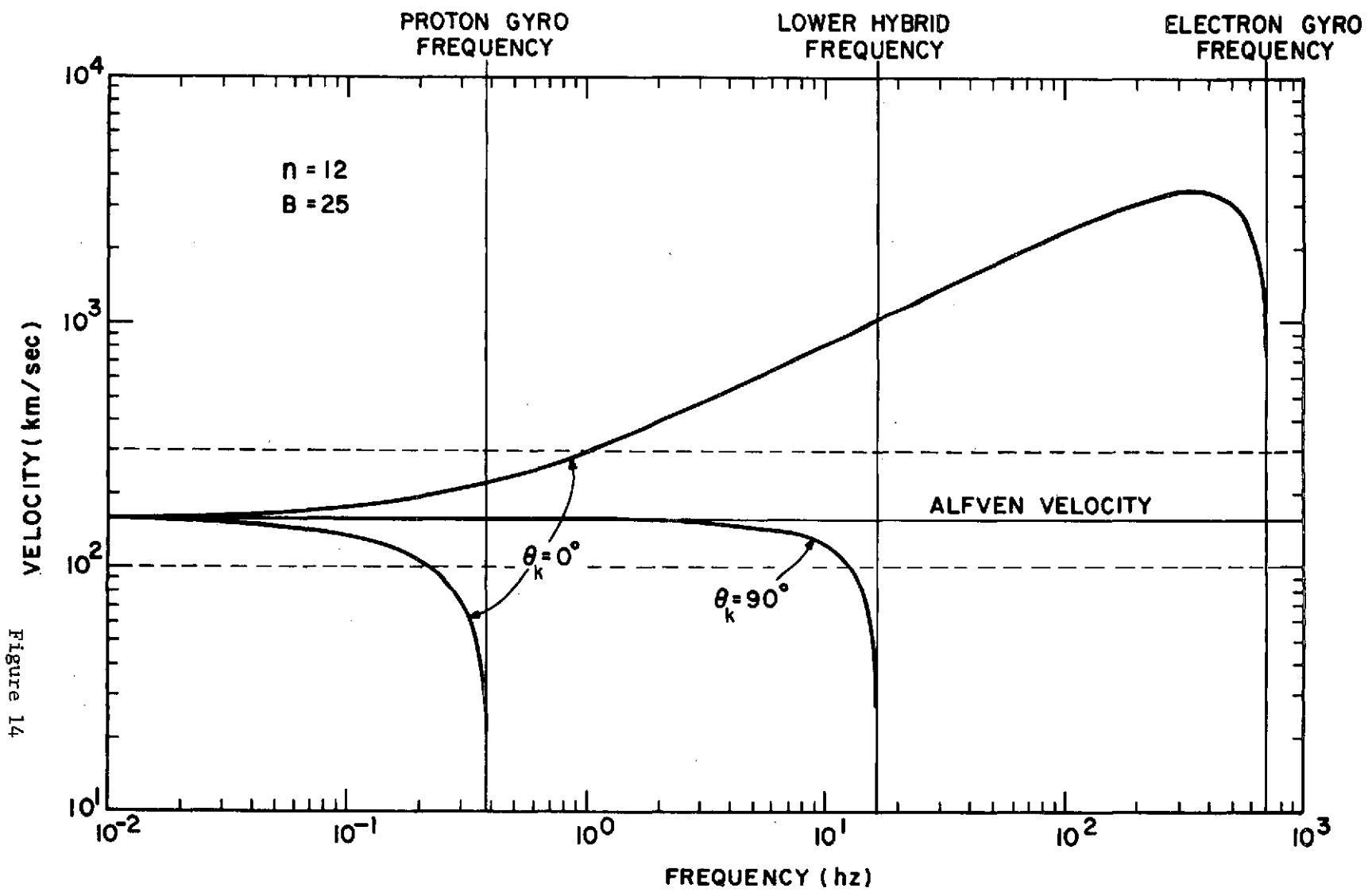
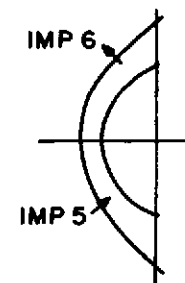


Figure 14

IMP 6	{	X <sub>SE</sub> = 7.1	8.5	9.8		11.0
		Y <sub>SE</sub> = -13.5	-14.8	-15.9		-16.9
		Z <sub>SE</sub> = 10.9	11.1	11.1		11.1
IMP 5	{	X <sub>SE</sub> = 12.5	11.3	9.9	8.3	
		Y <sub>SE</sub> = 12.9	11.6	10.1	8.5	
		Z <sub>SE</sub> = 7.8	7.8	7.8	7.5	

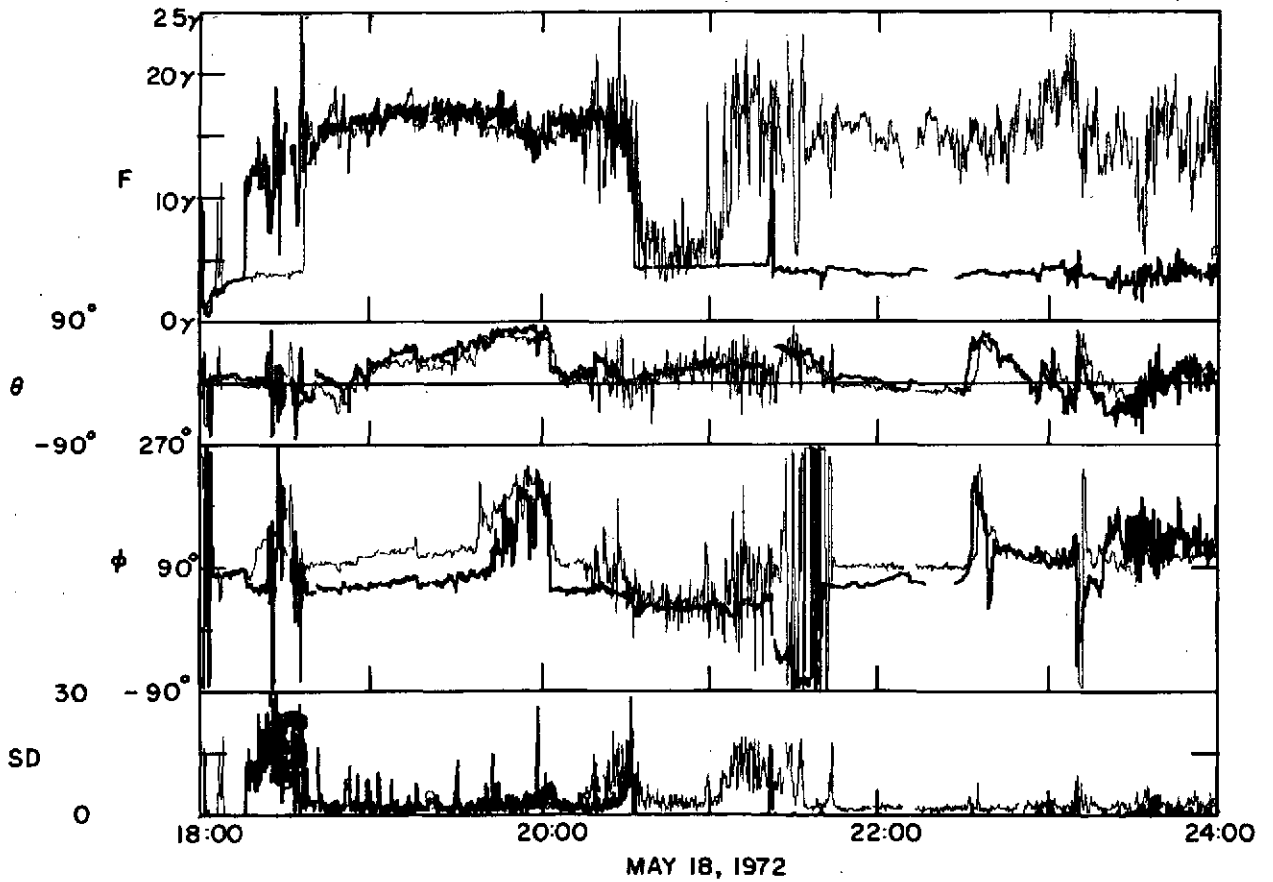


Figure 15

Figure 16

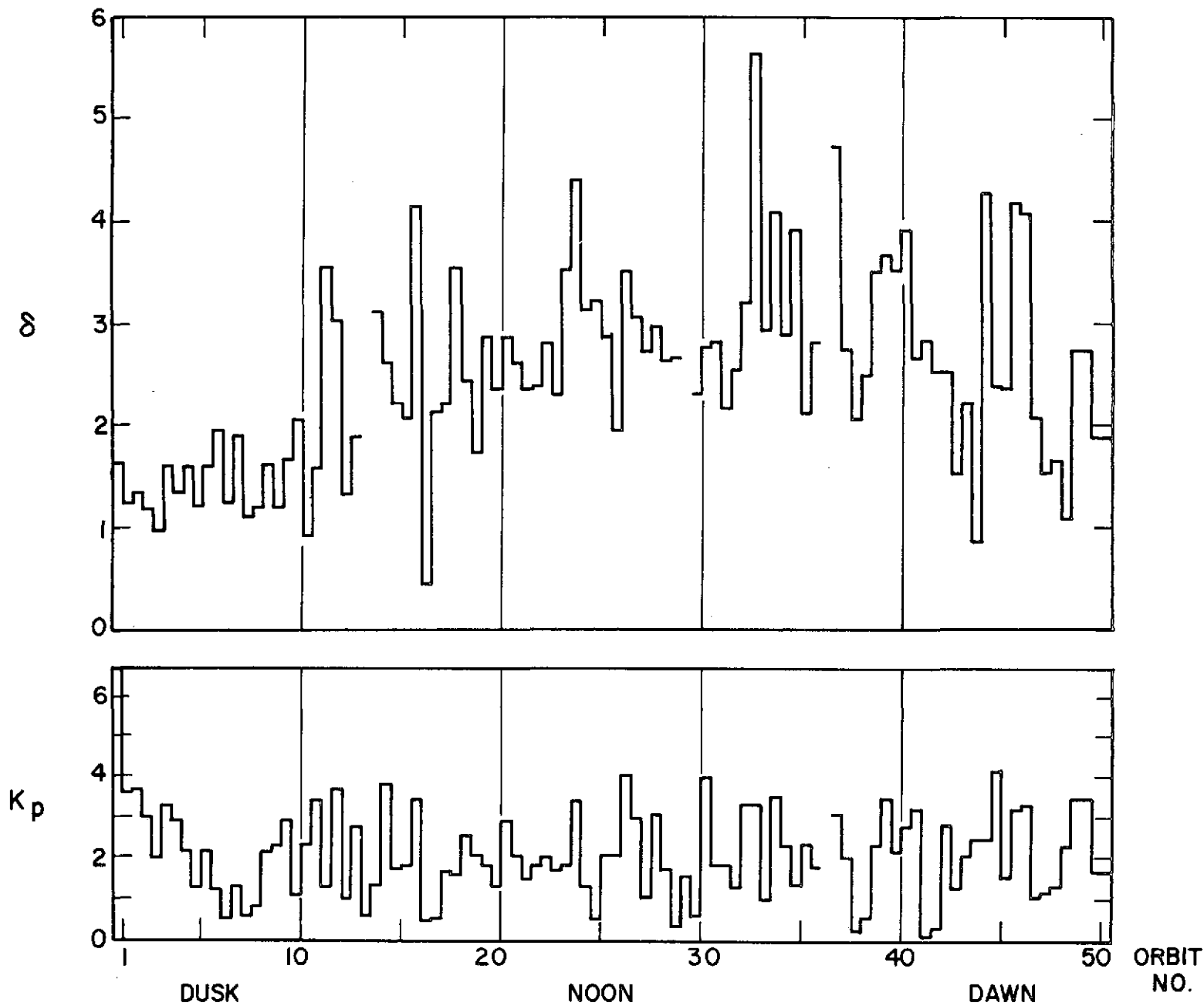
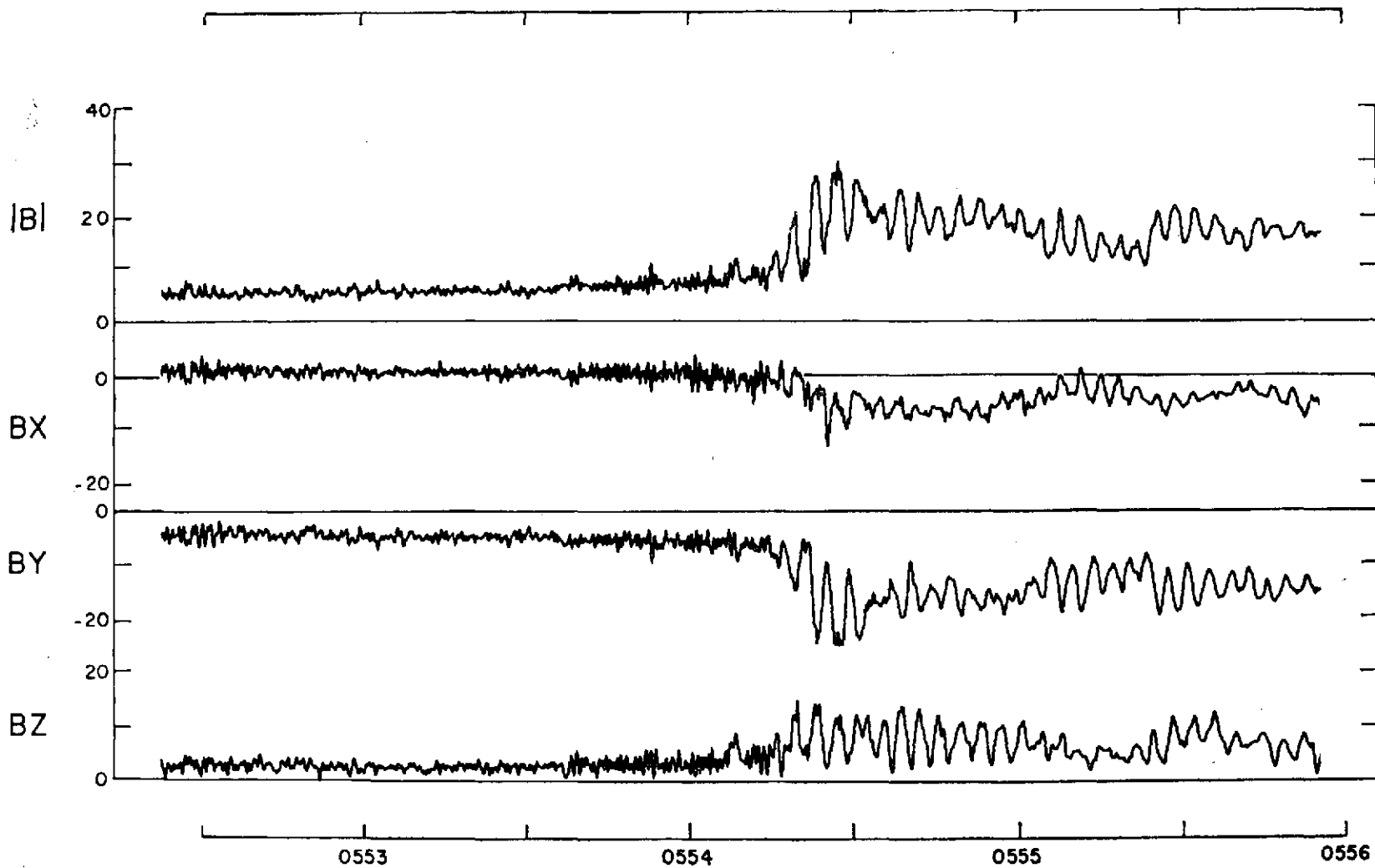


Figure 17



UNIVERSAL TIME